Author(s): S.M. Soskin, R. Mannella, O.M. Yevtushenko, I.A. Khovanov, P.V.E. McClintock
Chapter details: A New Approach to the Treatment of Separatrix Chaos and Its Applications, In: Hamitonian Chaos Beyond the KAM Theory, Dedicated to George M. Zaslavsky (1935—2008)

Year of publication: 2010
Link to published article: http://www.springer.com/new+&+forthcoming+titles+(default)/book/978-3-642-12717-5
Publisher statement: None

A New Approach To The Treatment Of Separatrix Chaos And Its Applications

S.M. Soskin, R. Mannella, O.M. Yevtushenko, I.A. Khovanov, P.V.E. McClintock

Abstract We consider time-periodically perturbed 1D Hamiltonian systems possessing one or more separatrices. If the perturbation is weak, then the separatrix chaos is most developed when the perturbation frequency lies in the logarithmically small or moderate ranges: this corresponds to the involvement of resonance dynamics into the separatrix chaos. We develop a method matching the discrete chaotic dynamics of the separatrix map and the continuous regular dynamics of the resonance Hamiltonian. The method has allowed us to solve the long-standing problem of an accurate description of the maximum of the separatrix chaotic layer width as a function of the perturbation frequency. It has also allowed us to predict and describe new phenomena including, in particular: (i) a drastic facilitation of the onset of global chaos between neighbouring separatrices, and (ii) a huge increase in the size of the low-dimensional stochastic web.

S.M. Soskin
Institute of Semiconductor Physics, 03028 Kiev, Ukraine,
e-mail: ssoskin@ictp.it

R. Mannella
Dipartimento di Fisica, Università di Pisa, 56127 Pisa, Italy,
e-mail: mannella@df.unipi.it

O.M. Yevtushenko
Physics Department, Ludwig-Maximilians-Universität München, D-80333 München, Germany,
e-mail: bom@ictp.it

I.A. Khovanov
School of Engineering, University of Warwick, Coventry CV4 7AL, UK,
e-mail: i.khovanov@warwick.ac.uk

P.V.E. McClintock
Physics Department, Lancaster University, Lancaster LA1 4YB, UK,
e-mail: p.v.e.mcclintock@lancaster.ac.uk

Contents[1]

1 Introduction

Separatrix chaos is the germ of Hamiltonian chaos [51]. Consider an integrable Hamiltonian system possessing a saddle, i.e. a hyperbolic point in the one-dimensional case, or a hyperbolic invariant torus, in higher-dimensional cases. The stable (incoming) and unstable (outgoing) manifolds of the saddle are called *separatrices* [18]: they separate trajectories that have different phase space topologies. If a weak time-periodic perturbation is added, then the separatrix is destroyed; it is replaced by a *separatrix chaotic layer* (SCL) [51, 18, 23, 29]. Even if the unperturbed system

[1] This version of the chapter represents just about 1/3 of the text in order to accord the copyright of the publisher. The presented parts are in bold in the contents.

does not possess a separatrix, the resonant part of the perturbation generates a separatrix in the auxiliary resonance phase space while the non-resonant part of the perturbation destroys this separatrix, replacing it with a chaotic layer [51, 18, 23, 10]. Thus separatrix chaos is of a fundamental importance for Hamiltonian chaos.

One of the most important characteristics of SCL is its width in energy (or expressed in related quantities). It can be easily found *numerically* by integration of the Hamiltonian equations with a set of initial conditions in the vicinity of the separatrix: the space occupied by the chaotic trajectory in the Poincaré section has a higher dimension than that for a regular trajectory, e.g. in the 3/2D case the regular trajectories lie on lines i.e. 1D objects while the chaotic trajectory lies within the SCL i.e. the object outer boundaries of which limit a 2D area.

On the other hand, it is important to be able to describe *theoretically* both the outer boundaries of the SCL and its width. There is a long and rich history of the such studies. The results may be classified as follows.

1.1 Heuristic results

Consider a 1D Hamiltonian system perturbed by a weak time-periodic perturbation:

$$\begin{aligned} &H = H_0(p,q) + hV(p,q,t), \\ &V(p,q,t+2\pi/\omega_f) = V(p,q,t), \qquad h \ll 1, \end{aligned} \tag{1}$$

where $H_0(p,q)$ possesses a separatrix and, for the sake of notational compactness, all relevant parameters of H_0 and V, except possibly for ω_f, are assumed to be ~ 1.

Physicists proposed a number of different heuristic criteria [53, 10, 23, 55, 51, 52] for the SCL width ΔE in terms of energy $E \equiv H_0(p,q)$ which gave qualitatively similar results:

$$\begin{aligned} &\Delta E \equiv \Delta E(\omega_f) \sim \omega_f \delta, \\ &\delta \equiv h|\varepsilon|, \\ &|\varepsilon| \lesssim 1 \qquad\qquad\qquad\qquad \text{for} \quad \omega_f \lesssim 1, \\ &|\varepsilon| \propto \exp(-a\omega_f) \ll 1 \qquad (a \sim 1) \qquad \text{for} \quad \omega_f \gg 1. \end{aligned} \tag{2}$$

The quantity $\delta \equiv h|\varepsilon|$ is called the *separatrix split* [51] (see also Eq. (4) below): it determines the maximum distance between the perturbed incoming and outgoing separatrices [53, 10, 23, 55, 51, 52, 1, 18, 29].

It follows from (2) that the maximum of ΔE should lie in the frequency range $\omega_f \sim 1$ while the maximum itself should be $\sim h$:

$$\Delta E_{\max} \equiv \max_{\omega_f}\{\Delta E(\omega_f)\} \sim h, \qquad \omega_f^{(\max)} \sim 1. \tag{3}$$

1.2 Mathematical and accurate physical results

Many papers studied the SCL by mathematical or accurate physical methods.

For the range $\omega_f \gg 1$, many works studied the separatrix splitting (see the review [18] and references therein) and the SCL width in terms of normal coordinates (see the review [29] and references therein). Though quantities studied in these works differ from those typically studied by physicists [53, 10, 23, 55, 51, 52], they implicitly confirm the main qualitative conclusion from the heuristic formula (2) in the high frequency range: provided that $\omega_f \gg 1$ the SCL width is exponentially small.

There were also several works studying the SCL in the opposite (i.e. adiabatic) limit $\omega_f \to 0$: see e.g. [27, 14, 28, 42, 45] and references therein. In the context of the SCL width, it is most important that $\Delta E(\omega_f \to 0) \sim h$ for most of the systems [27, 14, 28]. For a particular class of systems, namely for ac-driven spatially periodic systems (e.g. the ac-driven pendulum), the width of the SCL part above the separatrix diverges in the adiabatic limit [42, 45]: the divergence develops for $\omega_f \ll 1/\ln(1/h)$.

Finally, there is a qualitative estimation of the SCL width for the range $\omega_f \sim 1$ within the Kolmogorov-Arnold-Moser (KAM) theory [29]. The quantitative estimate within the KAM theory is lacking, apparently being very difficult for this frequency range [17]. It follows from the results in [29] that the width in this range is of the order of the separatrix split, which itself is of the order of h.

Thus it could seem to follow that, for all systems except ac-driven spatially periodic systems, the maximum in the SCL width is $\sim h$ and occurs in the range $\omega_f \sim 1$, very much in agreement with the heuristic result (3). Even for ac-driven spatially periodic systems, this conclusion could seem to apply to the width of the SCL part below the separatrix over the whole frequency range, and to the width of the SCL part above the separatrix for $\omega_f \gtrsim 1/\ln(1/h)$.

1.3 Numerical evidence for high peaks in $\Delta E(\omega_f)$ and their rough estimation

The above conclusion disagrees with several numerical studies carried out during the last decade (see e.g. [42, 45, 34, 25, 40, 24, 47, 35]) which have revealed the existence of sharp peaks in $\Delta E(\omega_f)$ in the frequency range $1/\ln(1/h) \lesssim \omega_f \lesssim 1$ the heights of which greatly exceed h (see also Figs. 2, 3, 5, 6 below). Thus, the peaks represent the general *dominant feature* of the function $\Delta E(\omega_f)$. They were related by the authors of [34, 25, 40, 24, 47, 35] to the absorption of nonlinear resonances by the SCL. For some partial case, rough heuristic estimates for the position and magnitude of the peaks were made in [34, 35].

1.4 Accurate description of the peaks and of the related phenomena

Until recently, accurate analytic estimates for the peaks were lacking. It is explicitly stated in [24] that the search for the mechanism through which resonances are involved in separatrix chaos, and for an accurate analytic description of the peaks in the SCL width as function of the perturbation frequency, are being among the most important and challenging tasks in the study of separatrix chaos. The first step towards accomplishing them was taken through the proposal [43, 44] of a new approach to the theoretical treatment of the separatrix chaos in the relevant frequency range. It was developed and applied to the onset of global chaos between two close separatrices. The application of the approach [43, 44] to the commoner single-separatrix case was also discussed. The approach has been further developed [38, 39], including an explicit theory for the single-separatrix case [39].

The present paper reviews the new approach [43, 44, 38, 39] and its applications to the single-separatrix [39] and double-separatrix [43, 44] cases. We also briefly review application to the enlargement of the low-dimensional stochastic web [46] and discuss other promising applications.

Though the form of our treatment differs from typical forms of mathematical theorems in this subject (cf. [18, 29]), it yields the *exact* expressions for the leading term in the relevant asymptotic expansions (the parameter of smallness is $\alpha \equiv 1/\ln(1/h)$) and, in some case, even for the next-order term. Our theory is in excellent agreement with results obtained by numerical integration of the equations of motion.

Sec. 2 describes the basic ideas underlying the approach. Sec. 3 is devoted to the leading-order asymptotic description of the single-separatrix chaotic layers. Sec. 4 presents an asymptotic description of the onset of global chaos in between two close separatrices. Sec. 5 describes the increase in sizes of a stochastic web. Conclusions are drawn in Sec. 6. Sec. 7 presents the Appendix, which explicitly matches the separatrix map and the resonance Hamiltonian descriptions for the double-separatrix case.

2 Basic ideas of the approach

The new approach [43, 44, 38, 39] may be formulated briefly as a matching between the discrete chaotic dynamics of the separatrix map in the immediate vicinity of the separatrix and the continuous regular dynamics of the resonance Hamiltonian beyond that region. The present section describes the general features of the approach in more detail.

Motion near the separatrix may be approximated by the *separatrix map* (SM) [53, 10, 23, 55, 51, 52, 1, 29, 34, 35, 43, 44, 31]. This was introduced in [53] and its various modifications were subsequently used in many studies. It is sometimes known as the *whisker map*. It was re-derived rigorously in [31] as the leading-order

approximation of motion near the separatrix in the asymptotic limit $h \to 0$, and an estimate of the error was also carried out in [31] (see also the review [29] and references therein).

The main ideas that allow one to introduce the SM [53, 10, 23, 55, 51, 52, 1, 29, 43, 44, 31] are as follows. For the sake of simplicity, let us consider a perturbation V that does not depend on the momentum: $V \equiv V(q,t)$. A system with energy close to the separatrix value spends most of its time in the vicinity of the saddle(s), where the velocity $\dot{q}$ is exponentially small. Differentiating $E \equiv H_0(p,q)$ with respect to time and allowing for the equations of motion of the system (1), we can show that $\mathrm{d}E/\mathrm{d}t \equiv \partial V/\partial q\dot{q} \propto \dot{q}$. Thus, the perturbation can significantly change the energy only when the velocity is not small i.e. during the relatively short intervals while the system is away from the saddle(s): these intervals correspond to *pulses* of velocity as a function of time (cf. Fig. 20 in the Appendix below). Consequently, it is possible to approximate the continuous Hamiltonian dynamics by a discrete dynamics which maps the energy E, the perturbation angle $\varphi \equiv \omega_f t$, and the velocity sign $\sigma \equiv \mathrm{sgn}(\dot{q})$, from pulse to pulse.

The actual form of the SM may vary, depending on the system under study, but its features relevant in the present context are similar for all systems. For the sake of clarity, consider the explicit case when the separatrix of $H_0(p,q)$ possesses a single saddle and two symmetric loops while $V = q\cos(\omega_f t)$. Then the SM reads [43] (cf. Appendix):

$$
\begin{aligned}
&E_{i+1} = E_i + \sigma_i h\varepsilon \sin(\varphi_i), \qquad (4)\\
&\varphi_{i+1} = \varphi_i + \frac{\omega_f \pi(3 - \mathrm{sgn}(E_{i+1} - E_s))}{2\omega(E_{i+1})},\\
&\sigma_{i+1} = \sigma_i \,\mathrm{sgn}(E_s - E_{i+1}), \qquad |\sigma_i| = 1,\\
&\qquad \varepsilon \equiv \varepsilon(\omega_f) = \mathrm{sgn}\left(\left.\frac{\partial H_0}{\partial p}\right|_{t\to-\infty} \right) \int_{-\infty}^{\infty} \mathrm{d}t \;\; \left.\frac{\partial H_0}{\partial p}\right|_{E_s} \sin(\omega_f t),\\
&\qquad E_i \equiv H_0(p,q)|_{t_i - \Delta}\,, \qquad \varphi_i \equiv \omega_f t_i, \qquad \sigma_i \equiv \mathrm{sgn}\left(\left.\frac{\partial H_0}{\partial p}\right|_{t_i} \right),
\end{aligned}
$$

where E_s is the separatrix energy, $\omega(E)$ is the frequency of oscillation with energy E in the unperturbed case (i.e. for $h = 0$), t_i is the instant corresponding to the i-th turning point in the trajectory $q(t)$ (cf. Fig. 20 in the Appendix below), and Δ is an arbitrary value from the range of time intervals which greatly exceed the characteristic duration of the velocity pulse while being much smaller than the interval between the subsequent pulses [53, 10, 23, 55, 51, 52, 1, 29, 31]. Consider the two most general ideas of our approach.

1. If a trajectory of the SM includes a state with $E = E_s$ and an arbitrary φ and σ, then this trajectory is chaotic. Indeed, the angle φ of such a state is not correlated with the angle of the state at the previous step of the SM, due to the divergence of $\omega^{-1}(E \to E_s)$. Therefore, the angle at the previous step may deviate from a

multiple of 2π by an arbitrary value. Hence the energy of the state at the previous step may deviate from E_s by an arbitrary value within the interval $[-h|\varepsilon|, h|\varepsilon|]$. The velocity sign σ is not correlated with that at the previous step either[2]. Given that a regular trajectory of the SM cannot include a step where all three variables change random-like, we conclude that such a trajectory must be chaotic.

Though the above arguments may appear to be obvious, they cannot be considered a mathematically rigorous proof, so that the statement about the chaotic nature of the SM trajectory which includes any state with $E = E_s$ should be considered as a conjecture supported by the above arguments and by numerical iteration of the SM. Possibly, a mathematically rigorous proof should involve an analysis of the Lyapunov exponents for the SM (cf. [23]) but this appears to be a technically difficult problem. We emphasize however that a rigorous proof of the conjecture is not crucial for the validity of the main results of the present paper, namely for the *leading* terms in the asymptotic expressions describing (i) the peaks of the SCL width as a function of the perturbation frequency in the single-separatrix case, and (ii) the related quantities for the double-separatrix case. It will become obvious from the next item that, to derive the leading term, it is sufficient to know that the chaotic trajectory does visit areas of the phase space where the energy deviates from the separatrix by values of the order of the separatrix split $\delta \equiv h|\varepsilon|$, which is a widely accepted fact [53, 10, 23, 55, 51, 52, 1, 18, 29].

2. It is well known [53, 10, 23, 55, 51, 52, 1, 18, 29, 34, 35, 43, 44], that, at the leading-order approximation, the frequency of eigenoscillation as function of the energy near the separatrix is proportional to the reciprocal of the logarithmic factor

$$\omega(E) = \frac{b\pi\omega_0}{\ln\left(\frac{\Delta H}{|E-E_s|}\right)}, \quad b = \frac{3-\mathrm{sgn}(E-E_s)}{2}, \qquad (5)$$
$$|E-E_s| \ll \Delta H \equiv E_s - E_{st},$$

where E_{st} is the energy of the stable states.

Given that the argument of the logarithm is large in the relevant range of E, the function $\omega(E)$ is nearly constant for a substantial variation of the argument. Therefore, as the SM maps the state $(E_0 = E_s, \varphi_0, \sigma_0)$ onto the state with $E = E_1 \equiv E_s + \sigma_0 h\varepsilon\sin(\varphi_0)$, the value of $\omega(E)$ for the given $\mathrm{sgn}(\sigma_0\varepsilon\sin(\varphi_0))$ is nearly the same for most of the angles φ_0 (except in the vicinity of multiples of π),

$$\omega(E) \approx \omega_r^{(\pm)}, \qquad (6)$$

[2] Formally, $\mathrm{sgn}(E-E_s)$ is not defined for $E = E_s$ but, if to shift E from E_s for an infinitesemal value, $\mathrm{sgn}(E-E_s)$ acquires a value equal to either $+1$ or -1, depending on the sign of the shift. Given that σ_{i+1} is proportional to $\mathrm{sgn}(E_s - E_{i+1})$ while the latter is random-like (as it has been shown above), σ_{i+1} is not correlated with σ_i if $E_{i+1} = E_s \pm 0$.

$$\omega_r^{(\pm)} \equiv \omega(E_s \pm h), \qquad \mathrm{sgn}(\sigma_0 \varepsilon \sin(\varphi_0)) = \pm 1.$$

Moreover, if the deviation of the SM trajectory from the separatrix increases further, $\omega(E)$ remains close to $\omega_r^{(\pm)}$ provided the deviation is not too large, namely if $\ln(|E-E_s|/h) \ll \ln(\Delta H/h)$. If $\omega_f \lesssim \omega_r^{(\pm)}$, then the evolution of the SM (4) may be regular-like for a long time until the energy returns to the close vicinity of the separatrix, where the trajectory becomes chaotic. Such behavior is especially pronounced if the perturbation frequency is close to $\omega_r^{(+)}$ or $\omega_r^{(-)}$ or to one of their multiples of relatively low order: the resonance between the perturbation and the eigenoscillation gives rise to an accumulation of energy changes for many steps of the SM, which results in a deviation of E from E_s that greatly exceeds the separatrix split $h|\varepsilon|$. Consider a state at the boundary of the SCL. The deviation of energy of such a state from E_s depends on its position at the boundary. In turn, the maximum deviation is a function of ω_f. The latter function possesses the absolute maximum at ω_f close to $\omega_r^{(+)}$ or $\omega_r^{(-)}$ typically[3], for the upper or lower boundary of the SCL respectively. This corresponds to the absorption of the, respectively upper and lower, 1st-order nonlinear resonance by the SCL.

The second of these intuitive ideas has been explicitly confirmed [43] (see Appendix): in the relevant range of energies, the separatrix map has been shown to reduce to two differential equations which are identical to the equations of motion of the auxiliary resonance Hamiltonian describing the resonance dynamics in terms of the conventional canonically conjugate slow variables, action I and slow angle $\tilde{\psi} \equiv n\psi - \omega_f t$ where ψ is the angle variable [10, 23, 55, 51, 52, 1] (see Eq. (16) below) and n is the relevant resonance number i.e. the integer closest to the ratio $\omega_f/\omega_r^{(\pm)}$.

Thus the matching between the discrete chaotic dynamics of the SM and the continuous regular-like dynamics of the resonance Hamiltonian arises in the following way [43]. After the chaotic trajectory of the SM visits any state on the separatrix, the system transits in one step of the SM to a given upper or lower curve in the $I-\tilde{\psi}$ plane which has been called [43] the upper or lower *generalized separatrix split* (GSS) curve[4] respectively:

$$E = E_{GSS}^{(\pm)}(\tilde{\psi}) \equiv E_s \pm \delta|\sin(\tilde{\psi})|, \qquad \delta \equiv h|\varepsilon|, \tag{7}$$

where δ is the conventional separatrix split [51], ε is the amplitude of the Melnikov-like integral defined in Eq. (4) above (cf. [53, 10, 23, 55, 51, 52, 1, 18, 29, 34, 47,

[3] For the SM relating to ac-driven spatially periodic systems, the time during which the SM undergoes a regular-like evolution above the separatrix diverges in the adiabatic limit $\omega_f \to 0$ [45], and the width of the part of the SM layer above the separatrix diverges too. However, we do not consider this case here since it is irrelevant to the main subject of the present paper i.e. to the involvement of the resonance dynamics into the separatrix chaotic motion.

[4] The GSS curve corresponds to the step of the SM which follows the state with $E = E_s$, as described above.

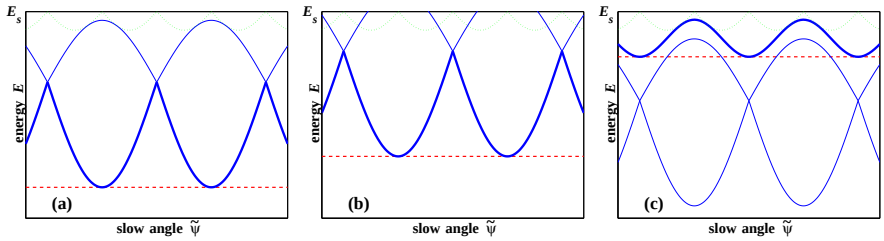

Fig. 1 Schematic figure illustrating the formation of the peak of the function $\Delta E_{sm}^{(-)}(\omega_f)$: (a) $\omega_f = \omega_{\max}$; (b) $\omega_f < \omega_{\max}$; (c) $\omega_f > \omega_{\max}$. The relevant (lower) GSS curve is shown by the dotted line. The relevant trajectories of the resonance Hamiltonian are shown by solid lines. The lower boundary of the layer is marked by a thick solid line: in (a) and (b) the lower boundary is formed by the lower part of the resonance separatrix while, in (c) it is formed by the resonance trajectory tangent to the GSS curve. The dashed line marks, for a given ω_f, the maximal deviation of the lower boundary from the separatrix energy E_s.

35, 43, 44]), and the angle $\tilde{\psi}$ may take any value either from the range $[0,\pi]$ or from the range $[\pi,2\pi]$[5].

After that, because of the closeness of ω_f to the n-th harmonic of $\omega(E)$ in the relevant range of E[6], for a relatively long time the system follows the *nonlinear resonance* (NR) dynamics (see Eq. (16) below), during the first half of which the deviation of the energy from the separatrix value grows, greatly exceeding δ for most of the trajectory. As time passes, $\tilde{\psi}$ is moving and, at some point, the growth of the deviation changes for the decrease. This decrease lasts until the system hits the GSS curve, after which it returns to the separatrix just for one step of the separatrix map. At the separatrix, the slow angle $\tilde{\psi}$ changes random-like, so that a new stage of evolution similar to the one just described occurs, i.e. the nonlinear resonance dynamics starting from the GSS curve with a new (random) value of $\tilde{\psi}$.

Of course, the SM cannot describe the variation of the energy during the velocity pulses (i.e. in between instants relevant to the SM): in some cases this variation can be comparable to the change within the SM dynamics. This additional variation will be taken into account below, where relevant.

One might argue that, even for the instants relevant to the SM, the SM describes the original Hamiltonian dynamics only approximately [31] and may therefore miss some fine details of the motion: for example, the above picture does not include small windows of stability on the separatrix itself. However these fine details are irrelevant in the present context, in particular the relative portion of the windows of stability on the separatrix apparently vanishes in the asymptotic limit $h \to 0$.

---

[5] Of these two intervals, the relevant one is that in which the derivative $\mathrm{d}E/\mathrm{d}t$ in the nonlinear resonance equations (see Eq. (16) below) is positive or negative, for the case of the upper or lower GSS curve respectively.

[6] I.e. E determined by Eq. (7) for any $\tilde{\psi}$ except from the vicinity of multiples of π. As shown in [43], Eq. (7) is irrelevant to the boundary of the chaotic layer in the range of $\tilde{\psi}$ close to multiples of π while the boundary in this range of $\tilde{\psi}$ still lies in the resonance range of energies, where $\omega(E) \approx \omega^{(\pm)}$.

The boundary of the SM chaotic layer is formed by those parts of the SM chaotic trajectory which deviate from the separatrix more than others. It follows from the structure of the chaotic trajectory described above that the upper/lower boundary of the SM chaotic layer is formed in one of the two following ways [43, 44]: (i) if there exists a *self-intersecting* resonance trajectory (in other words, the resonance separatrix) the lower/upper part of which (i.e. the part situated below/above the self-intersection) touches or intersects the upper/lower GSS curve while the upper/lower part does not, then the upper/lower boundary of the layer is formed by the upper/lower part of this self-intersecting trajectory (Figs. 1(a) and 1(b)); (ii) otherwise the boundary is formed by the resonance trajectory *tangent* to the GSS curve (Fig. 1(c)). It is shown below that, in both cases, the variation of the energy along the resonance trajectory is larger than the separatrix split δ by a logarithmically large factor $\propto \ln(1/h)$. Therefore, over the boundary of the SM chaotic layer the largest deviation of the energy from the separatrix value, $\Delta E_{sm}^{(\pm)}$, may be taken, in the leading-order approximation, to be equal to the largest variation of the energy along the resonance trajectory forming the boundary, while the latter trajectory can be entirely described within the resonance Hamiltonian formalism.

Finally, we mention that, as is obvious from the above description of the boundary, $\Delta E_{sm}^{(\pm)} \equiv \Delta E_{sm}^{(\pm)}(\omega_f)$ possesses a local maximum $\Delta E_{\max,sm}^{(\pm)}$ at ω_f for which the resonance separatrix just *touches* the corresponding GSS curve (see Fig. 1(a)).

3 Single-Separatrix Chaotic Layer

It is clear from Sec. 2 above that $\Delta E_{\max,sm}^{(\pm)}$ is equal in leading order to the width ΔE_{NR} of the nonlinear resonance which touches the separatrix. In Sec. 3.1 below, we *roughly* estimate ΔE_{NR} in order to classify two different types of systems. Secs. 3.2 and 3.3 present the *accurate* leading-order asymptotic theory for the two types of systems. The *next-order* correction is estimated in Sec. 3.4, while a *discussion* is presented in Sec. 3.5.

3.1 Rough estimates. Classification of systems.

Let us roughly estimate ΔE_{NR}: it will turn out that it is thus possible to classify all systems into two different types. With this aim, we expand the perturbation V into two Fourier series in t and in ψ respectively:

$$V \equiv \frac{1}{2}\sum_l V^{(l)}(E,\psi)\mathrm{e}^{-\mathrm{i}l\omega_f t} + \text{c.c.} \equiv \frac{1}{2}\sum_{l,k} V_k^{(l)}(E)\mathrm{e}^{\mathrm{i}(k\psi - l\omega_f t)} + \text{c.c.} \qquad (8)$$

As in standard nonlinear resonance theory [10, 23, 55, 51, 52], we single out the relevant (for a given peak) numbers K and L for the blind indices k and l respectively, and denote the absolute value of $V_K^{(L)}$ as V_0:

$$V_0(E) \equiv |V_K^{(L)}(E)|. \tag{9}$$

To estimate the width of the resonance roughly, we use the pendulum approximation of resonance dynamics [10, 23, 55, 51, 52, 1]:

$$\Delta E_{NR} \sim \sqrt{8hV_0\omega_f/|\mathrm{d}\omega/\mathrm{d}E|}. \tag{10}$$

This approximation assumes constancy of $\mathrm{d}\omega/\mathrm{d}E$ in the resonance range of energies, which is not the case here: in reality, $\omega(E) \propto 1/\ln(1/|E-E_s|)$ in the vicinity of the separatrix [53, 10, 23, 55, 51, 52, 1, 29, 34, 47, 35, 43, 44], so that the relevant derivative $|\mathrm{d}\omega/\mathrm{d}E| \sim (\omega_r^{(\pm)})^2/(\omega_0|E-E_s|)$ varies strongly within the resonance range. However, for our rough estimate we may use the maximal value of $|E-E_s|$, which is approximately equal to ΔE_{NR}. If ω_f is of the order of $\omega_r^{(\pm)} \sim \omega_0/\ln(1/h)$, then Eq. (10) reduces to the following approximate asymptotic equation for ΔE_{NR}:

$$\Delta E_{NR} \sim V_0(E = E_s \pm \Delta E_{NR})h\ln(1/h), \qquad h \to 0. \tag{11}$$

The asymptotic solution of Eq. (11) depends on $V_0(E_s \pm \Delta E_{NR})$ as a function of ΔE_{NR}. In this context, all systems can be divided in two types.

I The separatrix of the unperturbed system has *two or more* saddles while the relevant Fourier coefficient $V^{(L)} \equiv V^{(L)}(E,\psi)$ possesses *different* values on adjacent saddles. Given that, for $E \to E_s$, the system stays most of time near one of the saddles, the coefficient $V^{(L)}(E \to E_s, \psi)$ as a function of ψ is nearly a "square wave": it oscillates between the values at the different saddles. The relevant K is typically odd and, therefore, $V_0(E \to E_s)$ approaches a well defined non-zero value. Thus, the quantity $V_0(E = E_s \pm \Delta E_{NR})$ in Eq. (11) may be approximated by this non-zero limit, and we conclude therefore that

$$\Delta E_{NR} \propto h\ln(1/h), \qquad h \to 0. \tag{12}$$

II Either (i) the separatrix of the unperturbed system has a *single saddle*, or (ii) it has more than one saddle but the perturbation coefficient $V^{(L)}$ is *identical* for all saddles. Then $V^{(L)}(E \to E_s, \psi)$, as a periodic function of ψ, significantly differs from its value at the saddle(s) only during a small part of the period in ψ: this part is $\sim \omega(E)/\omega_0 \sim 1/\ln(1/|E_s-E|)$. Hence, $V_0(E_s \pm \Delta E_{NR}) \propto 1/\ln(1/\Delta E_{NR})$. Substituting this value in Eq. (11), we conclude that

$$\Delta E_{NR} \propto h, \qquad h \to 0. \tag{13}$$

Thus, for systems of type I, the maximum width of the SM chaotic layer is proportional to h times a logarithmically large factor $\propto \ln(1/h)$ while, for systems of type II, it is proportional to h times a numerical factor.

As shown below, the variation of energy in between the instants relevant to the SM is $\sim h$, i.e. much less than ΔE_{NR} (12) for systems of the type I, and of the same order as ΔE_{NR} (13) for systems of type II. Therefore, one may expect that the maximum width of the layer for the original Hamiltonian system (1), $\Delta E^{(\pm)}$, is at least roughly approximated by that for the SM, $\Delta E_{sm}^{(\pm)}$, so that the above classification of systems is relevant to $\Delta E^{(\pm)}$ too. This is confirmed both by numerical integration of the equations of motion of the original Hamiltonian system and by the accurate theory presented in the next two sub-sections.

3.2 Asymptotic theory for systems of type I.

For the sake of clarity, we consider a particular example of a type I system; its generalization is straightforward.

We choose an archetypal example: the ac-driven pendulum (sometimes referred to as a pendulum subject to a dipole time-periodic perturbation) [55, 42, 45]:

$$H = H_0 + hV, \tag{14}$$
$$H_0 = \frac{p^2}{2} - \cos(q), \qquad V = -q\cos(\omega_f t), \qquad h \ll 1.$$

Fig. 2 presents the results of numerical simulations for a few values of h and several values of ω_f. It shows that: (i) the function $\Delta E^{(-)}(\omega_f)$ indeed possesses sharp peaks whose heights greatly exceed the estimates by the heuristic [55], adiabatic [14] and moderate-frequency [29] theories (see inset); (ii) as predicted by our rough estimates of Sec. 3.1, the 1st peak of $\Delta E^{(-)}(\omega_f)$ shifts to smaller values of ω_f while its magnitude grows, as h decreases. Below, we develop a leading-order asymptotic theory, in which the parameter of smallness is $1/\ln(1/h)$, and compare it with results of the simulations.

Before moving on, we note that the SM (approximated in the relevant case by nonlinear resonance dynamics) considers states of the system only at discrete instants. Apart from the variation of energy within the SM dynamics, a variation of energy in the Hamiltonian system also occurs in between the instants relevant to the SM. Given that $\omega_f \ll 1$, this latter variation may be considered in adiabatic approximation and it is of the order of h [14, 35]. It follows from the above rough estimates, and from the more accurate consideration below, that the variation of energy within the SM dynamics for systems of type I is logarithmically larger i.e. larger by the factor $\ln(1/h)$. The variation of energy in between the instants relevant to the SM may therefore be neglected to leading-order for systems of type I: $\Delta E^{(-)} \simeq \Delta E_{sm}^{(-)}$. For the sake of notational compactness, we shall henceforth omit the subscript "*sm*" in this subsection.

For the system (14), the separatrix energy is equal to 1, while the asymptotic (for $E \to E_s$) dependence $\omega(E)$ is [55]:

$$\omega(E) \simeq \frac{\pi}{\ln(32/|E_s - E|)}, \qquad (15)$$
$$E_s = 1, \qquad |E_s - E| \ll 1.$$

Let us consider the range of energies below E_s (the range above E_s may be considered in an analogous way) and assume that ω_f is close to an odd multiple of $\omega_r^{(-)}$. The nonlinear resonance dynamics of the slow variables in the range of approximately resonant energies may be described as follows [43, 41] (cf. also [10, 23, 55, 51, 52, 1]):

$$\frac{\mathrm{d}I}{\mathrm{d}t} = -\frac{\partial \tilde{H}(I,\tilde{\psi})}{\partial \tilde{\psi}}, \qquad \frac{\mathrm{d}\tilde{\psi}}{\mathrm{d}t} = \frac{\partial \tilde{H}(I,\tilde{\psi})}{\partial I}, \qquad (16)$$
$$\tilde{H}(I,\tilde{\psi}) = \int_{I(E_s)}^{I} \mathrm{d}\tilde{I}\,(n\omega - \omega_f) \; - \; nhq_n \cos(\tilde{\psi})$$
$$\equiv n(E - E_s) - \omega_f (I - I(E_s)) \; - \; nhq_n \cos(\tilde{\psi})\,,$$

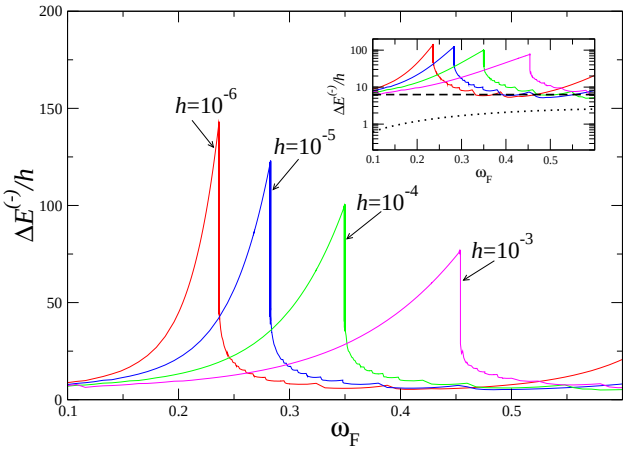

Fig. 2 Computer simulations for the ac driven pendulum (14) (an archetypal example of type I): the deviation $\Delta E^{(-)}$ of the lower boundary of the chaotic layer from the separatrix, normalized by the perturbation amplitude h, is plotted as a function of the perturbation frequency ω_f, for various h. The inset presents the same data but with a logarithmic ordinate and with the estimates by the heuristic [55], adiabatic [14] and moderate-frequency [29] theories. The heuristic estimate is shown by the dotted line: as an example of the heuristic estimate, we use the formula from [55]: $\Delta E^{(-)}/h = 2\pi\omega_f/\cosh(\pi\omega_f/2)$. The adiabatic and moderate-frequency estimates are shown by the dashed line: the adiabatic estimate for $\Delta E^{(-)}(\omega_f)$ is equal approximately to 2π; the estimate following from the results of the work [29] for $\omega_f \sim 1$ is of the same order, so that it is schematically represented in the inset in Fig. 2 by the same line as for the adiabatic estimate (dashed line). The inset shows explicitly that the simulation results exceed the estimates of the former theories by 1 or 2 orders of magnitude, over a wide range of frequencies.

$$
\begin{aligned}
&I \equiv I(E) = \int_{E_{\min}}^{E} \frac{\mathrm{d}\tilde{E}}{\omega(\tilde{E})}, \qquad E \equiv H_0(p,q),\\
&\tilde{\psi} = n\psi - \omega_f t,\\
&\psi = \pi + \mathrm{sign}(p)\omega(E)\int_{q_{\min}(E)}^{q} \frac{\mathrm{d}\tilde{q}}{\sqrt{2(E-U(\tilde{q}))}} + 2\pi l,\\
&q_n \equiv q_n(E) = \frac{1}{2\pi}\int_0^{2\pi} \mathrm{d}\psi\, q(E,\psi)\cos(n\psi),\\
&|n\omega - \omega_f| \ll \omega, \qquad n \equiv 2j-1, \qquad j = 1,2,3,\ldots,
\end{aligned}
$$

where I and ψ are the canonical variables action and angle respectively [10, 23, 55, 51, 52, 1]; $E_{\min}$ is the minimal energy over all q,p, $E \equiv H_0(p,q)$; $q_{\min}(E)$ is the minimum coordinate of the conservative motion with a given value of energy E; l is the number of right turning points in the trajectory $[q(\tau)]$ of the conservative motion with energy E and given initial state (q_0,p_0).

The resonance Hamiltonian $\tilde{H}(I,\tilde{\psi})$ is obtained in the following way. First, the original Hamiltonian H is transformed to action-angle variables $I-\psi$. Then it is multiplied by n and the term $\omega_f I$ is extracted (the latter two operations correspond to the transformation $\psi \to \tilde{\psi} \equiv n\psi - \omega_f t$). Finally, the result is being averaged over time i.e. only the resonance term in the double Fourier expansion of the perturbation is kept (it may be done since the effect of the fast-oscillating terms on the dynamics of slow variables is small: see the estimate of the corrections in Sec. 3.4 below).

Let us derive asymptotic expression for $I(E)$, substituting the asymptotic expression (15) for $\omega(E)$ into the definition of $I(E)$ (16) and carrying out the integration:

$$
I(E) \simeq I(E_s) - \frac{E_s - E}{\pi}\left(\ln\left(\frac{32}{E_s-E}\right)+1\right). \tag{17}
$$

As for the asymptotic value $q_n(E \to E_s)$, it can be seen that $q(E \to E_s, \psi)$, as a function of ψ, asymptotically approaches a "square wave", oscillating between $-\pi$ and π, so that, for sufficiently small j,

$$
\begin{aligned}
&q_{2j-1}(E \to E_s) \simeq (-1)^{j+1}\frac{2}{2j-1},\\
&q_{2j} = 0,\\
&j = 1,2,\ldots \ll \frac{\pi}{2\omega(E)}.
\end{aligned} \tag{18}
$$

The next issue is the analysis of the phase space of the resonant Hamiltonian (16). Substituting $\tilde{H}$ (16) into the equations of motion (16), it can be seen that their stationary points have the following values of the slow angle

$$
\tilde{\psi}_+ = \pi, \qquad \tilde{\psi}_- = 0, \tag{19}
$$

while the corresponding action is determined by the equation

$$n\omega - \omega_f \mp nh\frac{\mathrm{d}q_n}{\mathrm{d}I} = 0, \qquad n \equiv 2j-1, \tag{20}$$

where the sign "$\mp$"corresponds to $\tilde{\psi}_{\mp}$ (19).

The term $\propto h$ in (20) may be neglected to leading-order (cf. [10, 23, 55, 51, 52, 1, 43, 41]), and Eq. (20) reduces to the resonance condition

$$(2j-1)\omega(E_r^{(j)}) = \omega_f, \tag{21}$$

the lowest-order solution of which is

$$E_s - E_r^{(j)} \simeq 32\exp\left(-\frac{(2j-1)\pi}{\omega_f}\right). \tag{22}$$

Eqs. (19) and (22) together with (17) explicitly determine the elliptic and hyperbolic points of the Hamiltonian (16). The hyperbolic point is often referred to as a "saddle" and corresponds to $\tilde{\psi}_+$ or $\tilde{\psi}_-$ in (19) for even or odd j respectively. The saddle point generates the resonance separatrix. Using the asymptotic relations (17) and (18), we find that the resonance Hamiltonian (16) takes the following asymptotic value in the saddle:

$$\begin{aligned}\tilde{H}_{saddle} &\simeq \frac{E_s - E_r^{(j)}}{\pi}\omega_f - 2h \\ &\simeq \frac{\omega_f}{\pi}32\exp\left(-\frac{\pi(2j-1)}{\omega_f}\right) - 2h.\end{aligned} \tag{23}$$

The second asymptotic equality in (23) takes into account the relation (22).

As explained in Sec. 2 above, $\Delta E^{(-)}(\omega_f)$ possesses a local maximum at ω_f for which the resonance separatrix is tangent to the lower GSS curve (Fig. 1(a)). For the relevant frequency range $\omega_f \to 0$, the separatrix split (which represents the maximum deviation of the energy along the GSS curve from E_s) approaches the following value [55] in the asymptotic limit $h \to 0$

$$\delta \simeq 2\pi h, \qquad \omega_f \ll 1. \tag{24}$$

As shown below, the variation of energy along the relevant resonance trajectories is much larger. Therefore, in the leading-order approximation, the GSS curve may simply be replaced by the separatrix of the unperturbed system i.e. by the horizontal line $E = E_s$ or, equivalently, $I = I(E_s)$. Then the tangency occurs at $\tilde{\psi}$, shifted from the saddle by π, so that the condition of tangency is written as

$$\tilde{H}_{saddle} = \tilde{H}(I = I(E_s), \tilde{\psi} = \tilde{\psi}_{saddle} + \pi) \equiv 2h. \tag{25}$$

Substituting here $\tilde{H}_{saddle}$ (23), we finally obtain the following transcendental equation for $\omega_{\max}^{(j)}$:

$$x\exp(x) = \frac{8(2j-1)}{h}, \qquad x \equiv \frac{(2j-1)\pi}{\omega_{\max}^{(j)}}. \tag{26}$$

Fig. 3(b) demonstrates the excellent agreement between Eq. (26) and simulations of the Hamiltonian system over a wide range of h.

In the asymptotic limit $h \to 0$, the lowest-order explicit solution of Eq. (26) is

$$\omega_{\max}^{(j)} \simeq \frac{(2j-1)\pi}{\ln\left(\frac{8(2j-1)}{h}\right)}, \qquad j = 1,2,... \ll \ln\left(\frac{1}{h}\right). \tag{27}$$

As follows from Eq. (26), the value of $E_s - E_r^{(j)}$ (22) for $\omega_f = \omega_{\max}^{(j)}$ is

$$E_s - E_r^{(j)}(\omega_f = \omega_{\max}^{(j)}) = \frac{4\pi h}{\omega_{\max}^{(j)}}. \tag{28}$$

Its leading-order expression is:

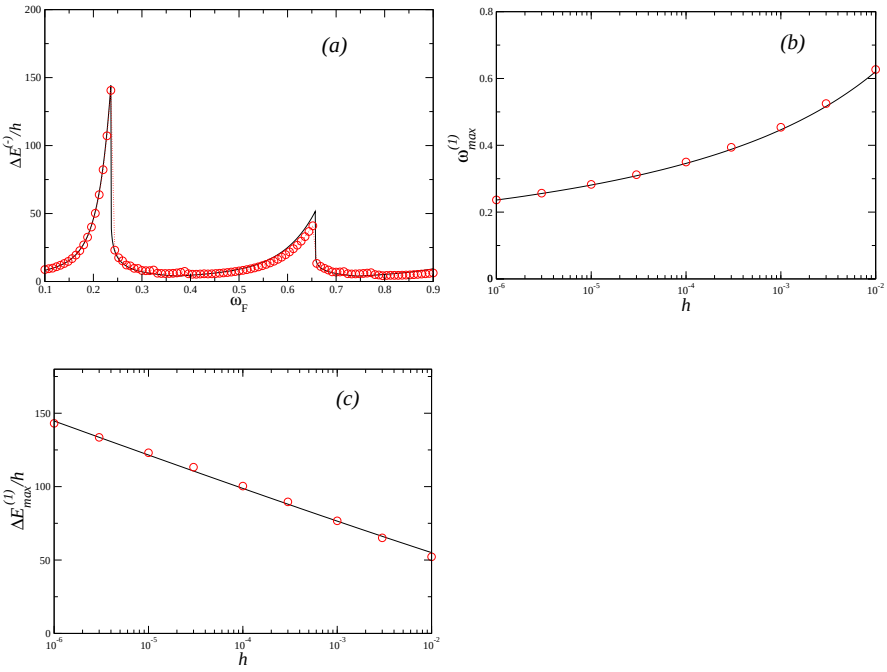

Fig. 3 An archetypal example of a type I system: the ac-driven pendulum (14). Comparison of theory (solid lines) and simulations (circles) for: (a) the deviation $\Delta E^{(-)}(\omega_f)$ of the lower boundary of the chaotic layer from the separatrix, normalized by the perturbation amplitude h, as a function of the perturbation frequency ω_f, for $h = 10^{-6}$; the theory is from Eqs. (26), (31), (32), (38), (39) and (41) (note the discontinuous drop by the factor e from the maximum to the right wing). (b) The frequency of the 1st maximum in $\Delta E^{(-)}(\omega_f)$ as a function of h; the theory is from Eq. (26). (c) The 1st maximum in $\Delta E^{(-)}(\omega_f)/h$ as a function of h; the theory is from Eqs. (34) and (26).

$$E_s - E_r^{(j)}(\omega_f = \omega_{\max}^{(j)}) \simeq \frac{4h}{2j-1} \ln\left(\frac{8(2j-1)}{h}\right), \qquad h \to 0. \tag{29}$$

If $\omega_f \leq \omega_{\max}^{(j)}$ then, in the chaotic layer, the largest deviation of energy from the separatrix value corresponds to the minimum energy $E_{\min}^{(j)}$ on the nonlinear resonance separatrix (Fig. 1(a,b)), which occurs at $\tilde{\psi}$ shifted by π from the saddle. The condition of equality of $\tilde{H}$ at the saddle and at the minimum of the resonance separatrix is written as

$$\tilde{H}_{saddle} = \tilde{H}(I(E_{\min}^{(j)}), \tilde{\psi}_{saddle} + \pi). \tag{30}$$

Let us seek its asymptotic solution in the form

$$E_s - E_{\min}^{(j)} \equiv \Delta E_l^{(j)} = (1+y)(E_s - E_r^{(j)}) \simeq (1+y)32\exp\left(-\frac{\pi(2j-1)}{\omega_f}\right),$$
$$y \gtrsim 1. \tag{31}$$

Substituting (31) and (23) into Eq. (30), we obtain for y the following transcendental equation:

$$(1+y)\ln(1+y) - y = \frac{h}{8(2j-1)} x_f \exp(x_f), \tag{32}$$
$$x_f \equiv \frac{\pi(2j-1)}{\omega_f}, \qquad \omega_f \leq \omega_{\max}^{(j)}, \qquad y > 0,$$

where $\omega_{\max}^{(j)}$ is given by Eq. (26).

Eqs. (31) and (32) describe the left wing of the j-th peak of $\Delta E^{(-)}(\omega_f)$. Fig. 3(a) demonstrates the good agreement between our analytic theory and simulations for the Hamiltonian system.

It follows from Eq. (26) that Eq. (32) for $\omega_f = \omega_{\max}^{(j)}$ reduces to the relation $\ln(1+y) = 1$, i.e.

$$1 + y(\omega_{\max}^{(j)}) = \mathrm{e}. \tag{33}$$

It follows from Eqs. (33), (31) and (28) that the maximum for a given peak is:

$$\Delta E_{\max}^{(j)} \equiv E_s - E_{\min}^{(j)}(\omega_{\max}^{(j)}) = \frac{4\pi \mathrm{e} h}{\omega_{\max}^{(j)}}. \tag{34}$$

Fig. 3(c) shows the excellent agreement of this expression with our simulations of the Hamiltonian system over a wide range of h.

The leading-order expression for $\Delta E_{\max}^{(j)}$ is:

$$\Delta E_{\max}^{(j)} \simeq \frac{4\mathrm{e}h}{2j-1} \ln(8(2j-1)/h), \qquad h \to 0, \tag{35}$$

which confirms the rough estimate (12).

As ω_f decreases, it follows from Eq. (32) that y increases exponentially sharply. In order to understand how $\Delta E_l^{(j)}$ decreases upon decreasing ω_f, it is convenient to rewrite Eq. (31) re-expressing the exponent by means of Eq. (32):

$$\Delta E_l^{(j)}(\omega_f) = \frac{4\pi h}{\omega_f(\ln(1+y) - y/(1+y))}. \tag{36}$$

It follows from Eqs. (32) and (36) that $\Delta E_l^{(j)}$ decreases *power-law-like* when ω_f is decreased. In particular, $\Delta E_l^{(j)} \propto 1/(\omega_{\max}^{(j)} - \omega_f)$ at the far part of the wing.

As for the right wing of the peak, i.e. for $\omega_f > \omega_{\max}^{(j)}$, over the chaotic layer, the largest deviation of energy from the separatrix value corresponds to the minimum of the resonance trajectory tangent to the GSS curve (Fig. 1(c)). The value of $\tilde{\psi}$ at the minimum coincides with $\tilde{\psi}_{saddle}$. In the leading-order approximation, the GSS curve may be replaced by the horizontal line $I = I(E_s)$, so that the tangency occurs at $\tilde{\psi} = \tilde{\psi}_{saddle} + \pi$. Then the energy at the minimum $E_{\min}^{(j)}$ can be found from the equation

$$\tilde{H}(I(E_s), \tilde{\psi}_{saddle} + \pi) = \tilde{H}(I(E_{\min}^{(j)}), \tilde{\psi}_{saddle}) \tag{37}$$

Let us seek its asymptotic solution in the form

$$E_s - E_{\min}^{(j)} \equiv \Delta E_r^{(j)} = z(E_s - E_r^{(j)}) \simeq z32\exp\left(-\frac{\pi(2j-1)}{\omega_f}\right)$$
$$0 < z < 1, \qquad z \sim 1. \tag{38}$$

Substituting (38) into (37), we obtain for z the following transcendental equation:

$$z(1+\ln(1/z)) = \frac{h}{8(2j-1)} x_f \exp(x_f) \tag{39}$$
$$x_f \equiv \frac{\pi(2j-1)}{\omega_f}, \qquad \omega_f > \omega_{\max}^{(j)}, \qquad 0 < z < 1,$$

where $\omega_{\max}^{(j)}$ is given by Eq. (26). Eqs. (38) and (39) describe the right wing of the j-th peak of $\Delta E^{(-)}(\omega_f)$. Fig. 3(a) demonstrates the good agreement between our analytic theory and simulations.

It follows from Eq. (26) that the solution of Eq. (39) for $\omega_f \to \omega_{\max}^{(j)}$ is $z \to 1$, so the right wing starts from the value given by Eq. (28) (or, approximately, by Eq. (29)). Expressing the exponent in (38) from (39), we obtain the following equation

$$\Delta E_r^{(j)}(\omega_f) = \frac{4\pi h}{\omega_f(1+\ln(1/z))}. \tag{40}$$

It follows from Eqs. (39) and (40) that $\Delta E_r^{(j)}$ decreases *power-law-like* for increasing ω_f. In particular, $\Delta E_r^{(j)} \propto 1/(\omega_f - \omega_{\max}^{(j)})$ in the far part of the wing. Further analysis of the asymptotic shape of the peak is presented in Sec. 3.5 below.

Beyond the peaks, the function $\Delta E^{(-)}(\omega_f)$ is logarithmically small in comparison with the maxima of the peaks. The functions $\Delta E_l^{(j)}(\omega_f)$ and $\Delta E_r^{(j)}(\omega_f)$ in the ranges beyond the peaks are also logarithmically small. Hence, nearly any function of $\Delta E_r^{(j)}(\omega_f)$ and $\Delta E_l^{(j+1)}(\omega_f)$ which is close to $\Delta E_r^{(j)}(\omega_f)$ in the vicinity of $\omega_{\max}^{(j)}$ and to $\Delta E_l^{(j+1)}(\omega_f)$ in the vicinity of $\omega_{\max}^{(j+1)}$ while being sufficiently small beyond the peaks may be considered as an approximation of the function $\Delta E^{(-)}(\omega_f)$ to logarithmic accuracy with respect to the maxima of the peaks, $\Delta E_{\max}^{(j)}$ and $\Delta E_{\max}^{(j+1)}$, in the whole range $[\omega_{\max}^{(j)}, \omega_{\max}^{(j+1)}]$. One of the easiest options is the following:

$$\begin{aligned}
&\Delta E^{(-)}(\omega_f) = \Delta E_l^{(1)}(\omega_f) && \text{for} \quad \omega_f < \omega_{\max}^{(1)}, \\
&\Delta E^{(-)}(\omega_f) = \max\{\Delta E_r^{(j)}(\omega_f), \Delta E_l^{(j+1)}(\omega_f)\} && \text{for} \quad \omega_{\max}^{(j)} < \omega_f < \omega_{\max}^{(j+1)}, \\
&j = 1, 2, \ldots \ll \frac{\pi}{2\omega_{\max}^{(1)}}. && (41)
\end{aligned}$$

We used this function in Fig. 3(a), and the analogous one will also be used in the other cases.

In fact, the theory may be generalized in such a way that Eq. (41) would approximate $\Delta E^{(-)}(\omega_f)$ well in the ranges far beyond the peaks with logarithmic accuracy, even with respect to $\Delta E^{(-)}(\omega_f)$ itself rather than to $\Delta E_{\max}^{(j)}$ only (cf. the next section). However, we do not do this in the present case, being interested primarily in the leading-order description of the peaks.

Finally, we demonstrate in Fig. 4 that the lowest-order theory describes the boundary of the layers quite well, even in the Poincaré section rather than only in energy/action.

3.3 Asymptotic theory for systems of type II.

We consider two characteristic examples of type II systems, corresponding to the classification given in Sec. 3.1. As an example of a system where the separatrix of the unperturbed system possesses a single saddle, we consider an ac-driven Duffing oscillator [1, 18, 29, 40]. As an example of the system where the separatrix possesses more than one saddle, while the perturbation takes equal values at the saddles, we consider a pendulum with an oscillating suspension point [1, 18, 29, 34, 35]. The treatment of these cases is similar in many respects to that presented in Sec. 3.2 above. So, we present it in less detail, emphasizing the differences.

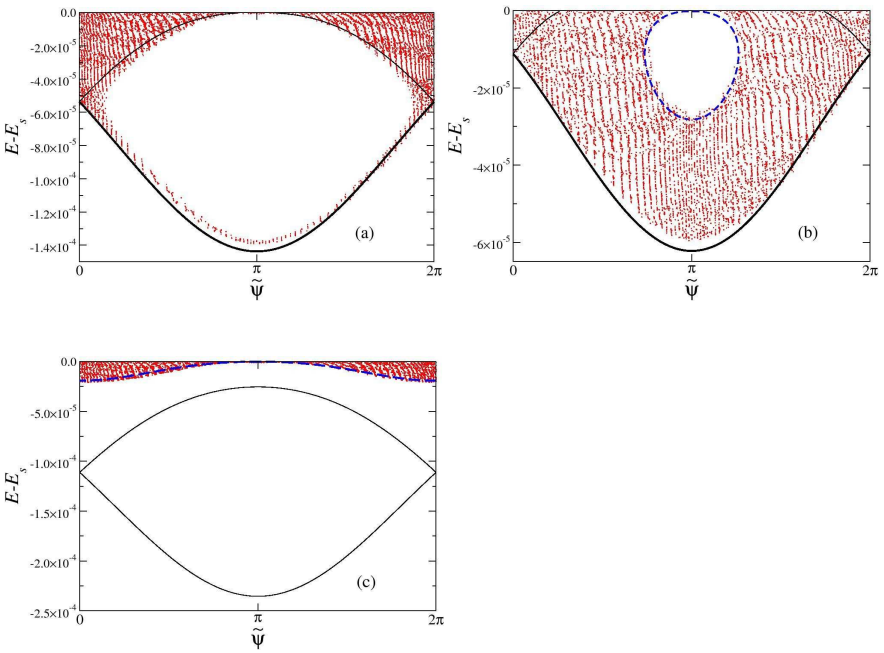

Fig. 4 Some characteristic Poincaré sections in the 2π-interval of the energy-angle plane for the system (14) with $h = 10^{-6}$ and ω_f equal to: (a) 0.236 (maximum), (b) 0.21 (left wing), (c) 0.25 (right wing). Results of the numerical integration of the equations of motion for the original Hamiltonian (14) are shown by (red) dots. The NR separatrix calculated in the leading-order approximation (i.e. by the integration of the resonant equations of motion (16) in which $\omega(E)$, $I(E)$ and $q_1(E)$ are approximated by the explicit formulæ (15), (17) and (18) respectively) is drawn by the (black) solid line. The NR trajectory (calculated in the leading-order approximation) tangent to the line $E = E_s$ is drawn by the (blue) dashed line. The outer boundary (marked by a thicker line) is approximated by: the lower part of the NR separatrix in cases (a) and (b), and by the tangent NR trajectory in case (c) The boundary of the island of stability in the cases (a) and (b) is approximated by the tangent NR trajectory (which coincides in the case (a) with the NR separatrix).

3.3.1 AC-driven Duffing oscillator.

Consider the following archetypal Hamiltonian [1, 18, 29, 40]:

$$H = H_0 + hV, \tag{42}$$
$$H_0 = \frac{p^2}{2} - \frac{q^2}{2} + \frac{q^4}{4}, \qquad V = -q\cos(\omega_f t), \qquad h \ll 1.$$

The asymptotic dependence of $\omega(E)$ on E for E below the separatrix energy $E_s = 0$ is the following [1, 13]

$$\omega(E) \simeq \frac{2\pi}{\ln(16/(E_s-E))}, \qquad E_s = 0, \qquad 0 < E_s - E \ll 1. \tag{43}$$

Correspondingly, the resonance values of energies (determined by the condition analogous to (21)) are

$$E_s - E_r^{(j)} = 16\exp\left(-\frac{2\pi j}{\omega_f}\right), \qquad j = 1,2,3,... \tag{44}$$

The asymptotic dependence of $I(E)$ is

$$I(E) \simeq I(E_s) - \frac{E_s - E}{2\pi}\left(\ln\left(\frac{16}{E_s-E}\right)+1\right). \tag{45}$$

The nonlinear resonance dynamics is described by the resonance Hamiltonian $\tilde{H}$ which is identical in form to Eq. (16). Obviously, the actual dependences $\omega(E)$ and $I(E)$ are given by Eq. (43) and (45) respectively. The most important difference is in $q_j(E)$: instead of a non-zero value (see (18)), it approaches 0 as $E \to E_s$. Namely, it is $\propto \omega(E)$ [1, 13]:

$$q_j(E) \simeq \frac{1}{\sqrt{2}}\omega(E), \qquad j = 1,2,... \ll \frac{\pi}{\omega(E)}, \tag{46}$$

i.e. q_j is much smaller than in systems of type I (cf. (18)). Due to this, the resonance is "weaker". At the same time, the separatrix split δ is also smaller, namely $\sim h\omega_f$ (cf. [43]) rather than $\sim h$ as for the systems of type I. That is why the separatrix chaotic layer is still dominated by resonance dynamics while the matching of the separatrix map and nonlinear resonance dynamics is still valid in the asymptotic limit $h \to 0$ [43].

Similarly to the previous section, we find the value of $\tilde{H}$ in the saddle in the leading-order approximation[7]:

$$\tilde{H}_{saddle} \simeq \omega_f\left(\frac{E_s - E_r^{(j)}}{2\pi} - \frac{h}{\sqrt{2}}\right), \tag{47}$$

where $E_s - E_r^{(j)}$ is given in (44).

As before, the maximum width of the layer corresponds to ω_f, for which the resonance separatrix is tangent to the GSS curve (Fig. 1(a)). It can be shown [43] that the angle of tangency asymptotically approaches $\tilde{\psi}_{saddle} + \pi = \pi$ while the energy still lies in the resonance range. Here $\omega(E) \approx \omega_r^{(-)} \approx \omega_f/j$. Using the expressions for $\tilde{H}(E,\tilde{\psi})$ (cf. (16)), $I(E)$ (45), $q_j(E)$ (46), and taking into account that in the tangency $E < \delta \sim h\omega_f \ll h$, to leading-order the value of $\tilde{H}$ at the tangency reads

[7] The only essential difference is that q_n at the saddle is described by Eq. (46) rather than by Eq. (18).

$$\tilde{H}_{tangency} \simeq \omega_f \frac{h}{\sqrt{2}}. \tag{48}$$

Allowing for Eqs. (47) and (48), the condition for the maximum, $\tilde{H}_{saddle} = \tilde{H}_{tangency}$, reduces to

$$E_s - E_r^{(j)}(\omega_{\max}^{(j)}) \simeq 2\pi\sqrt{2}h. \tag{49}$$

Thus these values $E_s - E_r^{(j)}$ are logarithmically smaller than the corresponding values (28) for systems of type I.

The values of ω_f corresponding to the maxima of the peaks in $\Delta E^{(-)}(\omega_f)$ are readily obtained from (49) and (44):

$$\omega_{\max}^{(j)} \simeq \frac{2\pi j}{\ln(4\sqrt{2}/(\pi h))}, \qquad j = 1,2,... \ll \ln(1/h). \tag{50}$$

The derivation to leading order of the shape of the peaks for the chaotic layer of the separatrix map, i.e. within the nonlinear resonance (NR) approximation, is similar to that for type I. So, we present only the results, marking them with the subscript "*NR*".

The left wing of the jth peak of $\Delta E_{NR}^{(-)}(\omega_f)$ is described by the function

$$\Delta E_{l,NR}^{(j)}(\omega_f) = 16(1+y)\exp\left(-\frac{2\pi j}{\omega_f}\right) \equiv \frac{2\pi\sqrt{2}h}{\ln(1+y) - y/(1+y)}, \tag{51}$$
$$\omega_f \le \omega_{\max}^{(j)},$$

where y is the positive solution of the transcendental equation

$$(1+y)\ln(1+y) - y = \frac{\pi h}{4\sqrt{2}}\exp\left(\frac{2\pi j}{\omega_f}\right), \qquad y > 0. \tag{52}$$

In common with the type I case, $1 + y(\omega_{\max}^{(j)}) = \mathrm{e}$, so that

$$\Delta E_{\max,NR}^{(j)} = \mathrm{e}(E_s - E_r^{(j)}(\omega_{\max}^{(j)})) \simeq 2\pi\mathrm{e}\sqrt{2}h. \tag{53}$$

Eq. (53) confirms the rough estimate (13). The right wing of the peak is described by the function

$$\Delta E_{r,NR}^{(j)}(\omega_f) = 16z\exp\left(-\frac{2\pi j}{\omega_f}\right) \equiv \frac{2\pi\sqrt{2}h}{1+\ln(1/z)}, \tag{54}$$
$$\omega_f > \omega_{\max}^{(j)},$$

where $z < 1$ is the solution of the transcendental equation

$$z(1+\ln(1/z)) = \frac{\pi h}{4\sqrt{2}} \exp\left(\frac{2\pi j}{\omega_f}\right), \qquad 0 < z < 1. \tag{55}$$

As in the type I case, $z(\omega_f \to \omega_{\max}^{(j)}) \to 1$.

It follows from Eqs. (49) and (53) that the typical variation of energy within the nonlinear resonance dynamics (that approximates the separatrix map dynamics) is $\propto h$. For the Hamiltonian system, the variation of energy in between the discrete instants corresponding to the separatrix map [55, 51, 52, 1, 43, 31] is also $\propto h$. Therefore, unlike the type I case, one needs to take it into account even at the leading-order approximation. Let us consider the right well of the Duffing potential (the results for the left well are identical), and denote by t_k the instant at which the energy E at a given k-th step of the separatrix map is taken: it corresponds to the beginning of the k-th pulse of velocity [55, 43] i.e. the corresponding q is close to a left turning point q_{ltp} in the trajectory $[q(\tau)]$. Let us also take into account that the relevant frequencies are small so that the adiabatic approximation may be used. Thus, the change of energy from t_k up to a given instant t during the following pulse of velocity ($t - t_k \sim 1$) may be calculated as

$$\begin{aligned} \Delta E &= \int_{t_k}^{t} \mathrm{d}\tau \dot{q} h \cos(\omega_f \tau) \simeq h\cos(\omega_f t_k) \int_{t_k}^{t} \mathrm{d}\tau \dot{q} \\ &= h\cos(\omega_f t_k)(q(t) - q_{ltp}) \end{aligned} \tag{56}$$

For the motion near the separatrix, the velocity pulse corresponds approximately to $\psi = 0$ (see the definition of ψ (16)). Thus, the corresponding slow angle is $\tilde{\psi} \equiv j\psi - \omega_f t_k \simeq -\omega_f t_k$.

For the left wing of the peak of $\Delta E^{(-)}(\omega_f)$ (including also the maximum of the peak), the boundary of the chaotic layer of the separatrix map is formed by the lower part of the NR separatrix. The minimum energy along this separatrix occurs at $\tilde{\psi} = \pi$. Taking this into account, and also noting that $\tilde{\psi} \simeq -\omega_f t_k$, we conclude that $\cos(\omega_f t_k) \simeq -1$. So, $\Delta E \leq 0$, i.e. it does lower the minimum energy of the layer of the Hamiltonian system. The maximum reduction occurs at the right turning point q_{rtp}:

$$\max(|\Delta E|) \simeq h(q_{rtp} - q_{ltp}) = \sqrt{2}h. \tag{57}$$

We conclude that the left wing of the j-th peak is described as follows:

$$\Delta E_l^{(j)}(\omega_f) \simeq \Delta E_{l,NR}^{(j)}(\omega_f) + \sqrt{2}h, \qquad \omega_f \leq \omega_{\max}^{(j)}, \tag{58}$$

where $\Delta E_{l,NR}^{(j)}(\omega_f)$ is given by Eqs. (51)-(52). In particular, the maximum of the peak is:

$$\Delta E_{\max}^{(j)} \simeq (2\pi \mathrm{e} + 1)\sqrt{2}h \approx 25.6h. \tag{59}$$

For the right wing of the peak, the minimum energy of the layer of the separatrix map occurs when $\tilde{\psi}$ coincides with $\tilde{\psi}_{saddle}$ (Fig. 1(c)) i.e. is equal to 0. As a result,

$\cos(\omega_f t_k) \simeq 1$ and, hence, $\Delta E \geq 0$. So, this variation cannot lower the minimum energy of the layer for the main part of the wing, i.e. for $\omega_f \leq \omega_{bend}^{(j)}$ where $\omega_{bend}^{(j)}$ is defined by the condition $\Delta E_{r,NR}^{(j)} = \max(|\Delta E|) \equiv \sqrt{2}h$. For $\omega_f > \omega_{bend}^{(j)}$, the minimal energy in the layer occurs at $\tilde{\psi} = \pi$, and it is determined exclusively by the variation of energy during the velocity pulse (the NR contribution is close to zero at such $\tilde{\psi}$). Thus, we conclude that there is a bending of the wing at $\omega_f = \omega_{bend}^{(j)}$:

$$\begin{aligned} &\Delta E_r^{(j)}(\omega_f) = \Delta E_{r,NR}^{(j)}(\omega_f), \qquad && \omega_{\max}^{(j)} < \omega_f \leq \omega_{bend}^{(j)}, \\ &\Delta E_r^{(j)}(\omega_f) = \sqrt{2}h, && \omega_f \geq \omega_{bend}^{(j)}, \\ &\omega_{bend}^{(j)} = \frac{2\pi j}{\ln(8\sqrt{2}/h) + 1 - 2\pi}, \end{aligned} \tag{60}$$

where $\Delta E_{r,NR}^{(j)}(\omega_f)$ is given by Eqs. (54) and (55).

Analogously to the previous case, $\Delta E^{(-)}(\omega_f)$ may be approximated over the whole frequency range by Eq. (41) with $\Delta E_l^{(j)}$ and $\Delta E_r^{(j)}$ given by Eqs. (58) and (60) respectively. Moreover, unlike the previous case, the theory also describes accurately the range far beyond the peaks: $\Delta E^{(-)}$ is dominated in this range by the velocity pulse contribution ΔE, which is accurately taken into account both by Eqs. (58) and (60).

Fig. 5 shows very reasonable agreement between the theory and simulations, especially for the 1st peak[8].

3.3.2 Pendulum with an oscillating suspension point

Consider the archetypal Hamiltonian [1, 18, 29, 34, 35]

$$\begin{aligned} &H = H_0 + hV, \\ &H_0 = \frac{p^2}{2} + \cos(q), \qquad V = -\cos(q)\cos(\omega_f t), \qquad h \ll 1. \end{aligned} \tag{61}$$

Though the treatment is similar to that used in the previous case, there are also characteristic differences. One of them is the following: although the resonance Hamiltonian is similar to the Hamiltonian (16), instead of the Fourier component

[8] The disagreement between theory and simulations for the magnitude of the 2nd peak is about three times larger than that for the 1st peak, so that the height of the 2nd peak is about 30% smaller than that calculated from the asymptotic theory. This occurs because, for the energies relevant to the 2nd peak, the deviation from the separatrix is much higher than that for the 1st peak. Due to the latter, the Fourier coefficient $q_2(E)$ for the relevant E is significantly smaller than that obtained from the asymptotic formula (42). In addition, the velocity pulse contribution ΔE also significantly decreases while the separatrix split increases as ω_f becomes ~ 1.

of the coordinate, q_n, there should be the Fourier component of $\cos(q)$, V_n, which can be shown to be:

$$V_{2j} \simeq (-1)^{j+1}\frac{4}{\pi}\omega(E), \qquad E_s - E \ll 1, \tag{62}$$
$$V_{2j-1} = 0,$$
$$j = 1,2,... \ll \frac{2\pi}{\omega(E)}, \qquad V_n \equiv \frac{1}{2\pi}\int_0^{2\pi} d\psi \cos(q)\cos(n\psi).$$

The description of the chaotic layer of the separatrix map at the lowest order, i.e. within the NR approximation, is similar to that for the ac-driven Duffing oscillator. So we present only the results, marking them with the subscript "*NR*".

The frequency of the maximum of a given j-th peak is:

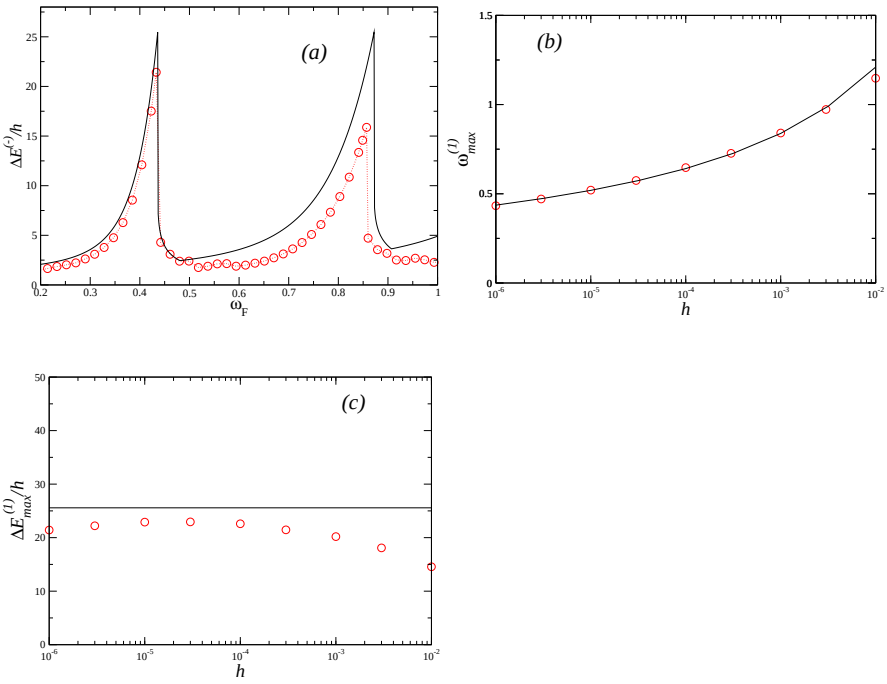

Fig. 5 An archetypal example of a type II system: the ac driven Duffing oscillator (42). Comparison of theory (solid lines) and simulations (circles): (a) the deviation $\Delta E^{(-)}(\omega_f)$ of the lower boundary of the chaotic layer from the separatrix, normalized by the perturbation amplitude h, as a function of the perturbation frequency ω_f, for $h = 10^{-6}$; the theory is from Eqs. (41), (50), (51), (52), (54), (55), (58) and (60) (note the discontinuous drop from the maximum to the right wing); (b) the frequency of the 1st maximum in $\Delta E^{(-)}(\omega_f)$ as a function of h; the theory is from Eq. (50); (c) the 1st maximum in $\Delta E^{(-)}(\omega_f)/h$ as a function of h; the theory is from Eq. (59).

$$\omega_{\max}^{(j)} \simeq \frac{2\pi j}{\ln(4/h)}, \qquad j = 1,2,... \ll \ln(4/h). \tag{63}$$

This expression agrees well with simulations for the Hamiltonian system (Fig. 6(b)). To logarithmic accuracy, Eq. (63) coincides with the formula following from Eq. (8) of [34] (reproduced in [35] as Eq. (21)) taken in the asymptotic limit $h \to 0$ (or, equivalently, $\omega_{\max}^{(j)} \to 0$). However, the numerical factor in the argument of the logarithm in the asymptotic formula following from the result of [34, 35] is half our value: this is because the nonlinear resonance is approximated in [34, 35] by the conventional pendulum model which is not valid near the separatrix (cf. our Sec. 3.1 above).

The left wing of the jth peak of $\Delta E_{NR}^{(-)}(\omega_f)$ is described by the function

$$\Delta E_{l,NR}^{(j)}(\omega_f) = 32(1+y)\exp\left(-\frac{2\pi j}{\omega_f}\right) \equiv \frac{8h}{\ln(1+y) - y/(1+y)}, \tag{64}$$
$$\omega_f \le \omega_{\max}^{(j)},$$

where y is the positive solution of the transcendental equation

$$(1+y)\ln(1+y) - y = \frac{h}{4}\exp\left(\frac{2\pi j}{\omega_f}\right), \qquad y > 0. \tag{65}$$

Similarly to the previous cases, $1 + y(\omega_{\max}^{(j)}) = \mathrm{e}$. Hence,

$$\Delta E_{\max,NR}^{(j)} = \mathrm{e}(E_s - E_r^{(j)}(\omega_{\max}^{(j)})) = 8\mathrm{e}h. \tag{66}$$

Eq. (66) confirms the rough estimate (13). The right wing of the peak is described by the function

$$\Delta E_{r,NR}^{(j)}(\omega_f) = 32z\exp\left(-\frac{2\pi j}{\omega_f}\right) \equiv \frac{8h}{1+\ln(1/z)}, \tag{67}$$
$$\omega_f > \omega_{\max}^{(j)},$$

where $z < 1$ is the solution of the transcendental equation

$$z(1+\ln(1/z)) = \frac{h}{4}\exp\left(\frac{2\pi j}{\omega_f}\right), \qquad 0 < z < 1. \tag{68}$$

Similarly to the previous cases, $z(\omega_f \to \omega_{\max}^{(j)}) \to 1$.

Now consider the variation of energy during a velocity pulse. Though the final result looks quite similar to the case with a single saddle, its derivation has some characteristic differences, and we present it in detail. Unlike the case with a single saddle, the pulse may start close to either the left or the right turning point, and the sign of the velocity in such pulses is opposite [55, 43]. The angle ψ in the pulse is

close to $-\pi/2$ or $\pi/2$ respectively. So, let us calculate the change of energy from the beginning of the pulse, t_k, until a given instant t within the pulse:

$$\Delta E = -\int_{t_k}^{t} \mathrm{d}\tau \dot{q} h \partial V/\partial q = h\int_{t_k}^{t} \mathrm{d}\tau \dot{q}(-\sin(q)\cos(\omega_f \tau))$$
$$\simeq h\cos(\omega_f t_k)\int_{t_k}^{t} \mathrm{d}\tau \dot{q}(-\sin(q)) \simeq h\cos(\omega_f t_k)(\cos(q(t))-1). \qquad (69)$$

Here, the third equality assumes adiabaticity while the last equality takes into account that the turning points are close to the maxima of the potential i.e. close to a multiple of 2π (where the cosine is equal to 1).

The quantity ΔE (69) takes its maximal absolute value at $q = \pi$. So, we shall further consider

$$\Delta E_{\max} = -2h\cos(\omega_f t_k) \equiv -2h\cos(2j\psi_k - \tilde{\psi}_k) = (-1)^{j+1} 2h\cos(\tilde{\psi}_k). \qquad (70)$$

The last equality takes into account that, as mentioned above, the relevant ψ_k is either $-\pi/2$ or $\pi/2$. For the left wing, the value of $\tilde{\psi}$ at which the chaotic layer of the separatrix map possesses a minimal energy corresponds to the minimum of the resonance separatrix. It is equal to π or 0 if the Fourier coefficient V_{2j} is positive or negative, i.e. for odd or even j, respectively: see Eq. (63). Thus $\Delta E_{\max} = -2h$ for any j and, therefore, it does lower the minimal energy of the boundary. We conclude that

$$\Delta E_l^{(j)}(\omega_f) \simeq \Delta E_{l,NR}^{(j)}(\omega_f) + 2h, \qquad \omega_f \leq \omega_{\max}^{(j)}, \qquad (71)$$

where $\Delta E_{l,NR}^{(j)}(\omega_f)$ is given by Eqs. (64)-(65). In particular, the maximum of the peak is:

$$\Delta E_{\max}^{(j)} \simeq (4\mathrm{e}+1)2h \approx 23.7h. \qquad (72)$$

The expression (72) confirms the rough estimate (13) and agrees well with simulations (Fig. 6(c)). At the same time, it differs from the formula which can be obtained from Eq. (10) of [34] (using also Eqs. (1), (3), (8), (9) of [34]) in the asymptotic limit $h \to 0$: the latter gives for $\Delta E_{\max}^{(j)}$ the asymptotic value $32h$. Though this result [34] (referred to also in [35]) provides for the correct functional dependence on h, it is quantitatively incorrect because (i) it is based on the pendulum approximation of the nonlinear resonance while this approximation is invalid in the vicinity of the separatrix (see the discussion of this issue in Sec. 3.1 above), and (ii) it does not take into account the variation of energy during the velocity pulse.

The right wing, by analogy to the case of the Duffing oscillator, possesses a bend at $\omega_f = \omega_{bend}^{(j)}$ where $\Delta E_{r,NR}^{(j)} = |\Delta E_{\max}| \equiv 2h$, corresponding to the shift of the relevant $\tilde{\psi}$ for π. We conclude that:

$$\begin{aligned}
&\Delta E_r^{(j)}(\omega_f) = \Delta E_{r,NR}^{(j)}(\omega_f), && \omega_{\max}^{(j)} < \omega_f \le \omega_{bend}^{(j)},\\
&\Delta E_r^{(j)}(\omega_f) = 2h, && \omega_f \ge \omega_{bend}^{(j)},\\
&\omega_{bend}^{(j)} = \frac{2\pi j}{\ln(16/h) - 3}, && (73)
\end{aligned}$$

where $\Delta E_{r,NR}^{(j)}(\omega_f)$ is given by Eqs. (66) and (67).

Similarly to the previous case, both the peaks and the frequency ranges far beyond the peaks are well approximated by Eq. (41), with $\Delta E_l^{(j)}$ and $\Delta E_r^{(j)}$ given by Eqs. (71) and (73) respectively (Fig. 6(a)).

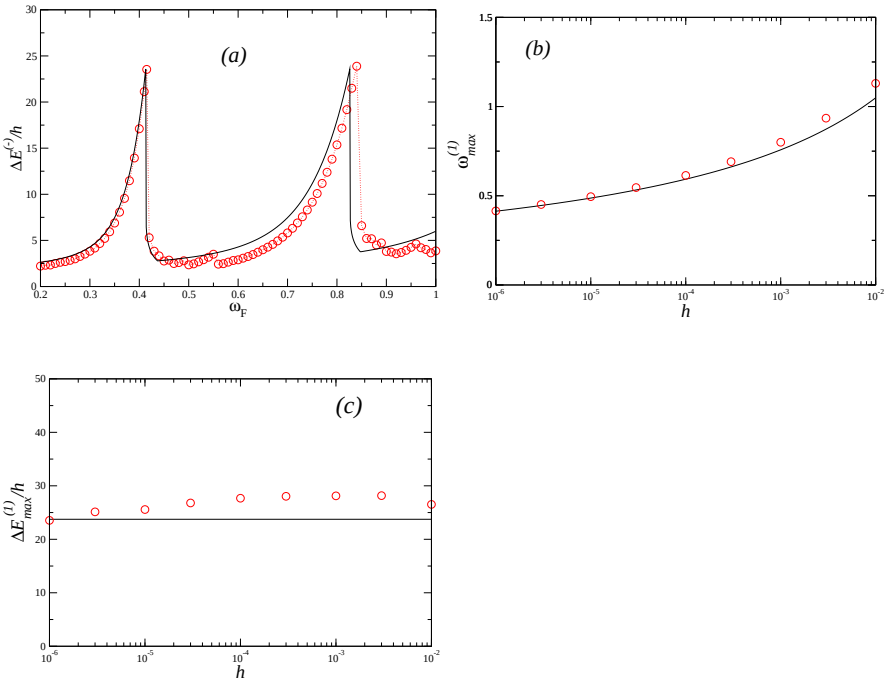

Fig. 6 An archetypal example of a type II system: the pendulum with an oscillating suspension point (61). Comparison of theory (solid lines) and simulations (circles): (a) The deviation $\Delta E^{(-)}(\omega_f)$ of the lower boundary of the chaotic layer from the separatrix, normalized by the perturbation amplitude h, as a function of the perturbation frequency ω_f, for $h = 10^{-6}$; the theory is by Eqs. (41), (63), (64), (65), (67), (68), (71) and (73) (note the discontinuous drop from the maximum to the right wing). (b) The frequency of the 1st maximum in $\Delta E^{(-)}(\omega_f)$ as a function of h; the theory is from Eq. (63). (c) The 1st maximum in $\Delta E^{(-)}(\omega_f)/h$ as a function of h; the theory is from Eq. (72).

3.4 Estimate of the next-order corrections

We have calculated explicitly only the leading term ΔE in the asymptotic expansion of the chaotic layer width. Explicit calculation of the next-order term $\Delta E^{(next)}$ is possible, but it is rather complicated and cumbersome: cf. the closely related case with two separatrices [43] (see also Sec. 4 below). In the present section, where the perturbation amplitude h in the numerical examples is 4 orders of magnitude smaller than that in [43], there is no particular need to calculate the next-order correction quantitatively. Let us estimate it, however, in order to demonstrate that its ratio to the leading term does vanish in the asymptotic limit $h \to 0$.

We shall consider separately the contribution $\Delta E_w^{(next)}$ stemming from the various corrections *within* the resonance approximation (16) and the contribution $\Delta E_t^{(next)}$ stemming from the corrections *to* the resonance approximation.

The former contribution may be estimated in a similar way to the case considered in [43]: it stems, in particular, from the deviation of the GSS curve from the separatrix (this deviation reaches δ at certain angles: see Eq. (7)) and from the difference between the exact resonance condition (20) and the approximate one (21). It can be shown that the absolute value of the ratio between $\Delta E_w^{(next)}$ and the leading term is logarithmically small (cf. [43]):

$$\frac{|\Delta E_w^{(next)}|}{\Delta E} \sim \frac{1}{\ln(1/h)}. \tag{74}$$

Let us turn to the analysis of the contribution $\Delta E_t^{(next)}$, i.e. the contribution stemming from the corrections to the resonance Hamiltonian (16). It is convenient to consider separately the cases of the left and right wings of the peak.

As described in Secs. 3.2 and 3.3 above, the left wing corresponds in the leading-order approximation to formation of the boundary of the layer by the *separatrix* of the resonance Hamiltonian (16). The resonance approximation (16) neglects time-periodic terms while the frequencies of oscillation of these terms greatly exceed the frequency of eigenoscillation of the resonance Hamiltonian (16) around its relevant elliptic point i.e. the elliptic point inside the area limited by the resonance separatrix. As is well known [18, 23, 29, 51, 52, 55], fast-oscillating terms acting on a system with a separatrix give rise to the onset of an *exponentially narrow* chaotic layer in place of the separatrix. In the present context, this means that the correction to the maximal action $\tilde{I}$ stemming from fast-oscillating corrections to the resonance Hamiltonian, i.e. $\Delta E_t^{(next)}$, is *exponentially small*, thus being negligible in comparison with the correction $\Delta E_w^{(next)}$ (see (74)).

The right wing, described in Secs. 3.2 and 3.3 above, corresponds in leading-order approximation to the formation of the boundary of the layer by the resonance trajectory *tangent* to the GSS curve. For the part of the right wing exponentially close in frequency to the frequency of the maximum, the tangent trajectory is close to the resonance separatrix, so that the correction stemming from fast-oscillating terms is exponentially small, similarly to the case of the left wing. As the frequency

further deviates from the frequency of the maximum, the tangent trajectory further deviates from the resonance separatrix and the correction $\Delta E_t^{(next)}$ differs from the exponentially small correction estimated above. It may be estimated in the following way.

It follows from the second-order approximation of the averaging method [5] that the fast-oscillating terms lead, in the second-order approximation, to the onset of additional terms $h^2 T_{\tilde{I}}(\tilde{I},\tilde{\psi})$ and $h^2 T_{\tilde{\psi}}(\tilde{I},\tilde{\psi})$ in the dynamic equations for slow variables $\tilde{I}$ and $\tilde{\psi}$ respectively, where $T_{\tilde{I}}(\tilde{I},\tilde{\psi})$ and $T_{\tilde{\psi}}(\tilde{I},\tilde{\psi})$ are of the order of the power-law-like function of $1/\ln(1/h)$ in the relevant range of $\tilde{I}$. The corresponding correction to the width of the chaotic layer in energy may be expressed as

$$\Delta E_t^{(next)} = \int_{t_{\min}}^{t_{\max}} \mathrm{d}t \; h^2 T_{\tilde{I}} \omega(\tilde{I}), \tag{75}$$

where $t_{\min}$ and $t_{\max}$ are instants corresponding to the minimum and maximum deviation of the tangent trajectory from the separatrix of the unperturbed system (cf. Figs. 1(c) and 4(c)). The interval $t_{\max} - t_{\min}$ may be estimated as follows:

$$t_{\max} - t_{\min} \sim \frac{\pi}{|<\dot{\tilde{\psi}}>|}, \tag{76}$$

where $<\dot{\tilde{\psi}}>$ is the value of $\dot{\tilde{\psi}}$ averaged over the tangent trajectory. It follows from (16) that

$$|<\dot{\tilde{\psi}}>| \sim \omega_f - \omega(E_s - \delta) \sim \frac{\omega(E_s-\delta)}{\ln(1/h)} \sim \frac{\omega_0}{\ln^2(1/h)}. \tag{77}$$

Taking together Eqs. (75)-(77) and allowing for the fact that $T_{\tilde{I}}$ is of the order of a power-law-like function of $1/\ln(1/h)$, we conclude that

$$\Delta E_t^{(next)} \sim h^2 P(\ln(1/h)), \tag{78}$$

where $P(x)$ is some power-law-like function.

The value $\Delta E_t^{(next)}$ is still asymptotically smaller than the absolute value of the correction within the resonance approximation, $|\Delta E_w^{(next)}|$, which is of the order of h or $h/\ln(1/h)$ for systems of type I or type II respectively.

Thus, we conclude that, both for the left and right wings of the peak, (i) the correction $\Delta E_t^{(next)}$ is determined by the correction within the resonance approximation $\Delta E_w^{(next)}$, and (ii) in the asymptotic limit $h \to 0$, the overall next-order correction is negligible in comparison with the leading term:

$$\frac{|\Delta E^{(next)}|}{\Delta E} \equiv \frac{|\Delta E_w^{(next)} + \Delta E_t^{(next)}|}{\Delta E} \approx \frac{|\Delta E_w^{(next)}|}{\Delta E} \sim \frac{1}{\ln(1/h)} \xrightarrow{h\to 0} 0. \tag{79}$$

This estimate well agrees with results in Figs. 3-6.

3.5 Discussion

In this section, we briefly discuss the following issues: (i) the *scaled* asymptotic shape of the peaks; (ii) peaks in the range of *moderate* frequencies; (iii) *jumps* in the amplitude dependence of the layer width; (iv) chaotic *transport*; (v) smaller peaks at *rational* frequencies; (vi) other separatrix maps; and (vii) an application to the onset of *global chaos*.

1. Let us analyse the scaled asymptotic shape of the peaks. We consider first systems of type I. The peaks are then described in the leading-order approximation exclusively within separatrix map dynamics (approximated, in turn, by the NR dynamics). It follows from Eqs. (32), (34), (36), (39) and (40) that most of the peak for given j can be written in the universal scaled form:

$$\Delta E^{(j)}(\omega_f) = \Delta E^{(j)}_{\max} S\left(\frac{\pi(2j-1)}{(\omega^{(j)}_{\max})^2}(\omega_f - \omega^{(j)}_{\max})\right), \tag{80}$$

where the universal function $S(\alpha)$ is strongly asymmetric:

$$\begin{aligned} &S(\alpha) = \begin{cases} S_l(\alpha) & \text{for} \quad \alpha \le 0, \\ S_r(\alpha) & \text{for} \quad \alpha > 0, \end{cases} \qquad (81)\\ &S_l(\alpha) = \frac{1}{\mathrm{e}(\ln(1+y) - y/(1+y))}, \qquad (1+y)\ln(1+y) - y = \exp(-\alpha), \\ &S_r(\alpha) = \frac{1}{\mathrm{e}(1+\ln(1/z))}, \qquad z(1+\ln(1/z)) = \exp(-\alpha). \end{aligned}$$

It is not difficult to show that

$$\begin{aligned} &S_l(\alpha=0) = 1, \qquad S_r(\alpha \to +0) = \mathrm{e}^{-1}, \qquad (82)\\ &\frac{\mathrm{d}S_l(\alpha=0)}{\mathrm{d}\alpha} = 1 - \mathrm{e}^{-1}, \quad \frac{\mathrm{d}S_r(\alpha \to +0)}{\mathrm{d}\alpha} \to -\infty, \\ &S(\alpha \to \pm\infty) \propto \frac{1}{|\alpha|}. \end{aligned}$$

Thus, the function $S(\alpha)$ is discontinuous at the maximum. To the left of the maximum, it approaches the far part of the wing (which decreases in a power-law-like way) relatively *slowly* while, to the right of the maximum, the function first drops *jump-wise* by a factor e and then *sharply* approaches the far part of the wing (which again decreases in a power-law-like way).
It follows from Eqs. (80), (81), (82) and (27) that the peaks are logarithmically narrow, i.e. the ratio of the half-width of the peak, $\Delta\omega^{(j)}$, to $\omega^{(j)}_{\max}$ is logarithmically small:

$$\frac{\Delta\omega^{(j)}}{\omega_{\max}^{(j)}} \sim \frac{1}{\ln\left(8(2j-1)/h\right)}. \tag{83}$$

We emphasize that the shape (81) is not restricted to the example (14): it is valid for any system of type I.

For systems of type II, contributions from the NR and from the variation of energy during the pulse of velocity, in relation to their h dependence, are formally of the same order but, numerically, the latter contribution is usually much smaller than the former. Thus, typically, the function (81) approximates well the properly scaled shape of the major part of the peak for systems of type II too.

2. The quantitative theory presented in the paper relates only to the peaks of *small* order n i.e. in the range of logarithmically small frequencies. At the same time, the magnitude of the peaks is still significant up to frequencies of order of one. This occurs because, for motion close to the separatrix, the order of magnitude of the Fourier coefficients remains the same up to logarithmically large numbers n. The shape of the peaks remains the same but their magnitude typically decreases (though in some cases, e.g. in case of the wave-like perturbation [23, 51, 52, 55] it may even increase in some range of frequencies). The quantitative description of this decrease, together with analyses of more sophisticated cases, requires a generalization of our theory.
3. Apart from the frequency dependence of the layer width, our theory is also relevant to amplitude dependence: it describes the jumps [40] in the dependence of the width on h and the transition between the jumps and the linear dependence. The values of h at which the jumps occur, $h_{jump}^{(j)}$, are determined by the same condition that determines $\omega_{\max}^{(j)}$ in the frequency dependence of the width. The formulæ relevant to the left wings of the peaks in the frequency dependence describe the ranges $h > h_{jump}^{(j)}$ while the formulæ relevant to the right wings describe the ranges $h < h_{jump}^{(j)}$.
4. Apart from the description of the boundaries, the approach allows us to describe *chaotic transport* within the layer. In particular, it allows us to describe quantitatively the effect of the stickiness of the chaotic trajectory to boundaries between the chaotic and regular areas of the phase space [51, 52]. Moreover, the presence of additional (resonance) saddles should give rise to an additional slowing down of the transport, despite a widening of the area of the phase space involved in the chaotic transport.
5. Our approach can be generalized in order to describe smaller peaks at non-integer rational frequencies i.e. $\omega_f \approx n/m\omega_r^{(\pm)}$ where n and m are integer numbers.
6. Apart from Hamiltonian systems of the one and a half degrees of freedom and corresponding Zaslavsky separatrix maps, our approach may be useful in the treatment of other chaotic systems and separatrix maps (see [29] for the most recent major review on various types of separatrix maps and related continuous chaotic systems).
7. Finally we note that, apart from systems with a separatrix, our work may be relevant to *nonlinear resonances* in any system. If the system is perturbed by a

weak time-periodic perturbation, then nonlinear resonances arise and their dynamics is described by the model of the auxiliary time-periodically perturbed pendulum [10, 23, 55, 51, 52, 1, 18]. If the original perturbation has a single harmonic, then the effective perturbation of the auxiliary pendulum is necessarily a high-frequency one, and chaotic layers associated with the resonances are exponentially narrow [10, 23, 55, 51, 52, 1, 18] while our results are irrelevant. But, if either the amplitude or the angle of the original perturbation is slowly modulated, or if there is an additional harmonic of a slightly shifted frequency, then the effective perturbation of the auxiliary pendulum is a low-frequency one [43] and the layers become much wider[9] while our theoretical approach becomes relevant. It may allow to find optimal parameters of the perturbation for the facilitation of the onset of global chaos associated with the overlap in energy between different-order nonlinear resonances [10]: the overlap may be expected to occur at a much smaller amplitude of perturbation in comparison with that one required for the overlap in case of a single-harmonic perturbation.

References

1. Abdullaev S.S.: Construction of Mappings for Hamiltonian Systems and Their Applications. Springer, Berlin, Heidelberg (2006).
2. Abramovitz M., Stegun I.: Handbook of Mathematical Functions. Dover, New York (1970).
3. Andronov A.A., Vitt A.A., Khaikin S.E.: Theory of Oscillators. Pergamon, Oxford (1966).
4. Arnold V.I.: Instability of dynamical systems with several degrees of freedom. Sov. Math. Dokl. **5**, 581–585 (1964).
5. Bogolyubov N.N., Mitropolsky Yu.A.: Asymptotic Methods in the Theory of Nonlinear Oscillators. Gordon and Breach, New York (1961).
6. Carmona H.A. et al.: Two dimensional electrons in a lateral magnetic superlattice. Phys. Rev. Lett. **74**, 3009–3012 (1995).
7. Chernikov A.A. et al.: Minimal chaos and stochastic webs. Nature **326**, 559–563 (1987).
8. Chernikov A.A. et al.: Some peculiarities of stochastic layer and stochastic web formation. Phys. Lett. A **122**, 39–46 (1987).
9. Chernikov A.A. et al.: Strong changing of adiabatic invariants, KAM-tori and web-tori. Phys. Lett. A **129**, 377–380 (1988).
10. Chirikov B.V.: A universal instability of many-dimensional oscillator systems. Phys. Rep. **52**, 263–379 (1979).
11. del-Castillo-Negrete D., Greene J.M., Morrison P.J.: Area-preserving non-twist maps: periodic orbits and transition to chaos. Physica D **61**, 1–23 (1996).
12. Dullin H.R., Meiss J.D., Sterling D.: Generic twistless bifurcations. Nonlinearity **13**, 203–224 (2000).
13. Dykman M.I., Soskin S.M., Krivoglaz M.A.: Spectral distribution of a nonlinear oscillator performing Brownian motion in a double-well potential. Physica A **133**, 53–73 (1985).
14. Elskens Y. and Escande D.F.: Slowly pulsating separatrices sweep homoclinic tangles where islands must be small: an extension of classical adiabatic theory. Nonlinearity **4**, 615–667 (1991).

[9] This should not be confused with the widening occuring with the separatrix chaotic layer in the *original* pendulum if an originally single-harmonic perturbation of a high frequency is completed by one more harmonic of a slightly shifted frequency: see [47] and references therein.

15. Fromhold T.M. et al.: Effects of stochastic webs on chaotic electron transport in semiconductor superlattices. Phys. Rev. Lett. **87**, 046803-1–046803-4 (2001).
16. Fromhold T.M. et al.: Chaotic electron diffusion through stochastic webs enhances current flow in superlattices. Nature **428**, 726–730 (2004).
17. Gelfreich V., private communication.
18. Gelfreich V.G., Lazutkin V.F.: Splitting of separatrices: perturbation theory and exponential smallness. Russian Math. Surveys **56**, 499–558 (2001).
19. Howard J.E. and Hohs S.M.: Stochasticity and reconnection in Hamiltonian systems. Phys. Rev. A **29**, 418–421 (1984).
20. Howard J.E. and Humpherys J.: Non-monotonic twist maps. Physica **D 80**, 256–276 (1995).
21. Landau L.D. and Lifshitz E.M.: Mechanics. Pergamon, London (1976).
22. Leonel E.D.: Corrugated Waveguide under Scaling Investigation. Phys. Rev. Lett. **98**, 114102-1–114102-4 (2007).
23. Lichtenberg A.J. and Lieberman M.A.: Regular and Stochastic Motion. Springer, New York (1992).
24. Luo A.C.J.: Nonlinear dynamics theory of stochastic layers in Hamiltonian systems. Appl. Mech. Rev. **57**, 161–172 (2004).
25. Luo A.C.J., Gu K., Han R.P.S.: Resonant-Separatrix Webs in Stochastic Layers of the Twin-Well Duffing Oscillator. Nonlinear Dyn. **19**, 37–48 (1999).
26. Morozov A.D.: Degenerate resonances in Hamiltonian systems with 3/2 degrees of freedom. Chaos **12**, 539–548 (2002).
27. Neishtadt A.I.: Change in adiabatic invariant at a separatrix. Sov. J. Plasma Phys. **12**, 568–573 (1986).
28. Neishtadt A.I., Sidorenko V.V., and Treschev D.V.: Stable periodic motions in the problem on passage trough a separatrix. Chaos **7**, 2–11 (1997).
29. Piftankin G.N., Treschev D.V.: Separatrix maps in Hamiltonian systems. Russian Math. Surveys **62**, 219–322 (2007).
30. Prants S.V., Budyansky M.V., Uleysky M.Yu., Zaslavsky G.M.: Chaotic mixing and transport in a meandering jet flow. Chaos **16**, 033117-1–033117-8 (2006).
31. Rom-Kedar V.: Transport rates of a class of two-dimensional maps and flows. Physica D **43**, 229–268 (1990).
32. Rom-Kedar V.: Homoclinic tangles – classification and applications. Nonlinearity **7**, 441–473 (1994).
33. Schmelcher P. and Shepelyansky D.L.: Chaotic and ballistic dynamics for two–dimensional electrons in periodic magnetic fields. Phys. Rev. B **49**, 7418–7423 (1994).
34. Shevchenko I.I.: Marginal resonances and intermittent Behavious in the motion in the vicinity of a separatrix. Phys. Scr. **57**, 185–191 (1998).
35. Shevchenko I.I.: The width of a chaotic layer. Phys. Lett. A **372**, 808–816 (2008).
36. Schmidt G.J.O.: Deterministic diffusion and magnetotransport in periodically modulated magnetic fields. Phys. Rev. B **47**, 13007–13010 (1993).
37. Soskin S.M., unpublished.
38. Soskin S.M. and Mannella R.: New Approach To The Treatment Of Separatrix Chaos. In: Macucci C. and Basso G. (eds.) Noise and Fluctuations: 20th International Conference on Noise and Fluctuations (ICNF-2009), AIP CONFERENCE PROCEEDINGS 1129, 25-28, American Institute of Physics, Melville, New York.
39. Soskin S.M., Mannella R.: Maximal width of the separatrix chaotic layer. Phys. Rev. E **80**, 066212-1–066212-17 (2009).
40. Soskin S.M., Mannella R., Arrayás M. and Silchenko A.N.: Strong enhancement of noise-induced escape by transient chaos. Phys. Rev. E **63**, 051111-1–051111-6 (2001).
41. Soskin S.M., Mannella R. and McClintock P.V.E.: Zero-Dispersion Phenomena in oscillatory systems. Phys. Rep. **373**, 247–409 (2003).
42. Soskin S.M., Yevtushenko O.M., Mannella R.: Divergence of the Chaotic Layer Width and Strong Acceleration of the Spatial Chaotic Transport in Periodic Systems Driven by an Adiabatic ac Force. Phys. Rev. Lett. **95**, 224101-1–224101-4 (2005).

43. Soskin S.M., Mannella R., Yevtushenko O.M.: Matching of separatrix map and resonant dynamics, with application to global chaos onset between separatrices. Phys. Rev. E **77**, 036221-1–036221-29 (2008).
44. Soskin S.M., Mannella R., Yevtushenko O.M.: Separatrix chaos: new approach to the theoretical treatment. In: Chandre C., Leoncini X., and Zaslavsky G. (eds.) Chaos, Complexity and Transport: Theory and Applications (Proceedings of the CCT-07), pp. 119-128. World Scientific, Singapore, (2008).
45. Soskin S.M., Yevtushenko O.M., Mannella R.: Adiabatic divergence of the chaotic layer width and acceleration of chaotic and noise-induced transport. Commun. Nonlinear Sci. Numer. Simulat. **15**, 16–23 (2010).
46. Soskin S.M., Khovanov I.A., Mannella R., McClintock P.V.E.: Enlargement of a low-dimensional stochastic web. In: Macucci C. and Basso G. (eds.) Noise and Fluctuations: 20th International Conference on Noise and Fluctuations (ICNF-2009), AIP CONFERENCE PROCEEDINGS 1129, 17-20, American Institute of Physics, Melville, New York; Soskin S. M., McClintock P. V. E., Fromhold, T. M., Khovanov I. A., and Mannella R.: Stochastic webs and quantum transport in superlattices: an introductory review, Contemporary Physics, **51**, 233–248 (2010).
47. Vecheslavov V.V.: Chaotic layer of a pendulum under low-and medium-frequency perturbations. Tech. Phys. **49**, 521–525 (2004).
48. Ye P.D. et al.: Electrons in a periodic magnetic field induced by a regular array of micromagnets. Phys. Rev. Lett. **74**, 3013-3016 (1995).
49. Yevtushenko O.M. and Richter K.: Effect of an ac electric field on chaotic electronic transport in a magnetic superlattice. Phys. Rev. B **57**, 14839–14842 (1998).
50. Yevtushenko O.M. and Richter K.: AC-driven anomalous stochastic diffusion and chaotic transport in magnetic superlattices. Physica **E 4**, 256–276 (1999).
51. Zaslavsky G.M.: Physics of Chaos in Hamiltonian systems, 2nd edn. Imperial Colledge Press, London (2007).
52. Zaslavsky G.M.: Hamiltonian Chaos and Fractional Dynamics. Oxford University Press, Oxford (2008).
53. Zaslavsky G.M. and Filonenko N.N.: Stochastic instability of trapped particles and conditions of application of the quasi-linear approximation. Sov. Phys. JETP **27**, 851–857 (1968).
54. Zaslavsky G.M. et al.: Stochastic web and diffusion of particles in a magnetic field. Sov. Phys. JETP **64**, 294–303 (1986).
55. Zaslavsky G.M., Sagdeev R.D., Usikov D.A. and Chernikov A.A.: Weak Chaos and Quasi-Regular Patterns. Cambridge University Press, Cambridge (1991).